E-b), whereas no remarkable change in insulin signal was observed in those cultured on plastic dish (Fig. 5E-c,E-d). The reduction of insulin signals were also observed in anti-β1 integrin antibody treated cells cultured on laminin-1 (data not shown). These results suggest that β1-integrins are involved in the stimulatory effect of Matrigel and laminin-1 on differentiation.

EFFECT OF BASEMENT MEMBRANE INVOLVES p38 MAP KINASE

Our previous studies demonstrated the involvement of p42/44MAPK and p38MAPK but not PI-3kinase and JNK in endocrine differentiation of AR42J cells [Furukawa et al., 1999; Kitamura et al., 2007]. Integrin exerts its cellular responses by regulating these intracellular signaling molecules [Mainiero et al., 2000; Bhowmic et al., 2001]. We therefore studied the effects of Matrigel on the phosphorylation of p38 and p42/44 MAP kinases during differentiation. As shown in Figure 6A, a relatively high amount of phosphorylated p38 was observed in cells cultured on Matrigel. In contrast, no remarkable differences in the amount of phosphorylated p42/44 MAP kinase were observed. Similar patterns of phosphorylations of p38 and p42/44 were also observed in the cells cultured on laminin-1 (data not shown). Additionally, when the cells were incubated with anti-β1 antibody, the increase in the amount of phosphorylated p38 MAP kinase induced by Matrigel was reduced (Fig. 6B). Also, addition of SB203580 attenuated Matrigel-induced activation of p38 MAP kinase (Fig. 6C) and completely blocked the expression of insulin.

EFFECT OF ECMS ON DIFFERENTIATION OF PANCREATIC DUCTAL CELLS

Finally, we addressed whether basement membrane affects differentiation of pancreatic ductal cells to insulin-producing cells in vitro. Ductal cells were cultured on Matrigel and treated with activin and BTC. Cells were incubated for 7 days and insulin content was measured. As depicted in Figure 7A, the expression of mRNA for insulin in cells cultured in Matrigel-coated dishes was markedly higher than those cultured on control dish. Similarly, the insulin content was increased in cells cultured on Matrigel-coated dishes (Fig. 7B). As shown in Figure 7C, the expression of Pax6 was upregulated in cells cultured on Matrigel-coated dishes. The increase in the insulin content was inhibited by anti-β1-integrin antibody (data not shown).

DISCUSSION

We showed that appropriate culture system promoted β-cell differentiation in both pancreatic progenitor-like cell lines and

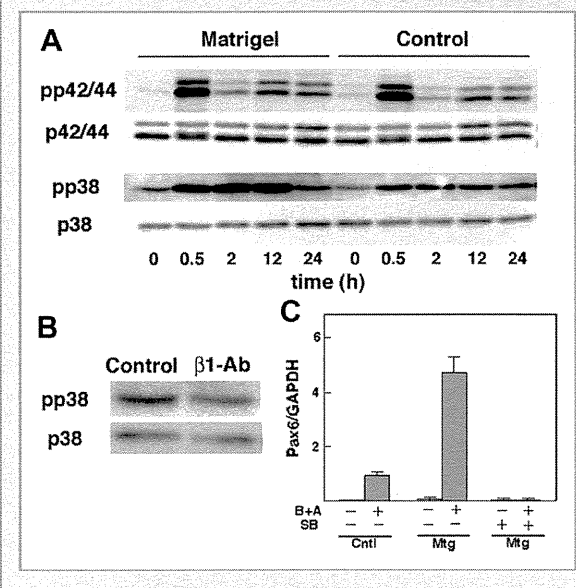

Fig. 6. Effect of matrigel on the activation of mitogen-activated kinases. A: Analysis of phosphorylation of p42/44 MAPK and p38 MAPK during differentiation. Cells cultured on matrigel or BSA (Control) were incubated for indicated time with a combination of activin A and BTC, and phosphorylation of p42/44 and p38 MAP kinases was analyzed by immnoblotting. B: Effect of anti-β1 integrin antibody on phosphorylation of p38 MAPK. Cells were preincubated with or without anti-β1 integrin antibody (β1 Ab) for 15 min and cultured on Matrigel in the presence of BTC and activin A. The cells were harvested 2 h after the treatment with BTC and activin A and Western blot analysis for p38 was performed. Typical images among the three independent analyses are shown. C: Effect of SB203580 on the expression of Pax6. Cells cultured on BSA-coated (Cntl) or Matrigel-coated (Mtrg) dishes were stimulated by activin A and BTC in the presence and absence of 10 μM SB203580 and the expression of Pax6 was measured by quantitative PCR.

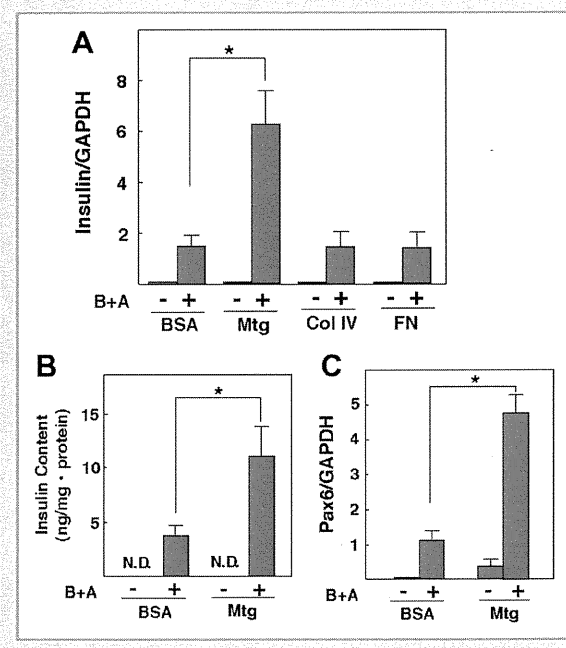

Fig. 7. Effect of ECM on differentiation of ductal cells. A: Expression of mRNA for insulin. Ductal cells were incubated for 7 days with 1 nM BTC and 2 nM activin A (B + A) in control-, Matrigel- (Mtg), collagen type IV- (col IV) and fibronectin-coated (FN) dishes. The expression of insulin was analyzed by real-time PCR. Results are shown as the mean ± SD for four experiments; $^*P < 0.05$. B: Changes in the insulin content. Ductal cells were incubated as indicated above and the insulin content was measured. Results are the mean ± SD for four experiments; $^*P < 0.05$. C: Changes in the expression of Pax6. Ductal cells were incubated with activin A and BTC for 48 h and the expression of Pax6 was measured by real-time PCR. Results are shown as the mean ± SD for four experiments; $^*P < 0.05$.

cultured duct epithelial cells. We found that Matrigel exerted the effect on β-cell differentiation through induction of Pax6, and the effect was reproduced at least partly by an individual ECM component, laminin-1. Additionally, using the blocking antibody we demonstrated that these favorable effects of basement membrane on β-cell differentiation were exerted through the interaction with β-1 integrin. Our data suggest that the basement membrane plays a crucial role in the regulation of β-cell differentiation and appropriate expression of transcriptional factors.

Several studies suggested the importance of the basement membrane in β-cell development [Lammert et al., 2001; Yoshitomi and Zaret, 2004]. In addition, the effectiveness of Matrigel in adult pancreatic duct cells and fetal pancreatic cells is reported [Jiang et al., 1999; Bonner-Weir et al., 2000]. These approaches using pancreatic explant may reflect physiological conditions, but it is unfavorable to study the molecular signalings due to heterogeneous cell population. In the present study, we used a simple model cell line reproducing β-cell differentiation. In agreement with previous studies, we demonstrated that reconstitute basement membrane, Matrigel was an effective substrate for differentiation in AR42J cells. Matrigel induced morphological changes and enhancement of the insulin expression during differentiation. Interestingly, we found the morphological changes comparable to those observed in activin-treated cells even in Matrigel-exposed cells without differentiation factors. Although Matrigel-exposed cells did not convert to endocrine cells expressing insulin or PP, these cells showed decrease in amylase expression in parallel with the increase in cytokeratin-20, a marker of pancreatic ductal cells (data not shown). Thus, Matrigel by itself may act on the initial step of differentiation although signals of differentiation factors are still required to convert to endocrine cells. This notion is supported by the concept that pancreatic progenitor cells in vivo are derived from ductal epithelium [Bonner-Weir and Weir, 2005]. In addition to enhancement of the insulin expression, Matrigel-exposed cells express more mature functions. This was evident by the following findings: upregulation of the expression of β-cell markers including SUR1, glucokinase and Pax6 [Sander et al., 1997; St-Onge et al., 1997; Ashery-Padan et al., 2001]; and intense and broadly cytoplasmic accumulation of insulin immunoreactivities. These results strongly suggest that the basement membrane component promotes differentiation. Our findings obtained in AR42J cells are advantageous in several respects compared to those of the previous data obtained in vivo and in vitro. In particular, since AR42J is a clonal cell line, they provide a good experimental system to study the regulation of differentiation and to identity the genes involved [Mashima et al., 1999; Kren et al., 2007]. Indeed, using this model system, we demonstrated the contribution of Pax6 (see below). Note that AR42J is slightly different from progenitors observed in vivo. For example, differentiated AR42J cells express low amount of insulin and lack some transcription factors including islet-1, Nkx6.1 and Maf A. Nonetheless, because we observed similar responsiveness to the basement membrane in ductal cells, AR42J is a useful model for investigating cellular signaling during β-cell differentiation.

Using this cell model, we addressed the intracellular signaling molecules involved in the basement membrane-induced enhancement of differentiation, in particular, the contribution of transcription factors. Of various transcription factors investigated, upregulation of Pax6 was demonstrated. This was observed only when cells were treated with differentiation factors and Matrigel, suggesting that cooperative signalings from extracellular matrix and growth factors are required for its expression. Interestingly, severe reduction of Pax6 expression in Xenopus embryonic endoderm is observed when the embryo is dissociated from the basement membrane of dorsal aorta [Lammert et al., 2001]. These findings strongly indicate that signals from the basement membrane are required for appropriate expression of transcription factor. We demonstrated the role of Pax6 in two ways: by a gain of function study and by a knockdown study. The gain of function study of Pax6 demonstrated up-regulation of insulin both in mRNA and protein levels. Overexpression of Pax6 also induced morphological changes comparable to these observed in Matrigel-exposed cells. However, Pax6-overexpressing cells also produced other hormones including glucagon and somatostatin. These findings indicate that induction of Pax6 reproduces differentiation-inducing activity of Matrigel, but the effect was not completely the same. The induction of glucagon and somatostatin in Pax6-overexpressing cells is not surprising since Pax6 also regulates transcription of these hormones as well as insulin [Sander et al., 1997; Cissell et al., 2003]. Unphysiologically excessive amounts of Pax6 may affect transcriptional regulation of these hormones. Consistent with this notion, we found a marked reduction of Pax4 and Nkx2.2 in Pax6-overexpressing cells (data not shown). Additionally, transgenic mice overexpressing Pax6 in islets exhibit glucagon and insulin double-positive cells and disruption of normal islet structures in the pancreas [Yamaoka et al., 2000]. In contrast to the results of the gain of function experiment, knockdown of Pax6 clearly attenuated upregulation of insulin and other β-cell markers. These effects were due to specific reduction of Pax6 since the expressions of other transcriptional factors were not changed. Taken together, Pax6 plays a key role in Matrigel-mediated differentiation in this model system. Pax6 is known to have a pleiotropic role in the development of the endocrine pancreas, and it is also thought to play an important role in α-, β-, δ-, and PP-cells [Sander et al., 1997; St-Onge et al., 1997]. With regard to the β-cell functions, Pax6 directly and indirectly regulates the expression of mature β-cell markers such as insulin, GLUT2, glucokinase, and IAPP [Sander et al., 1997; Ashery-Padan et al., 2001; Cissell et al., 2003]. However, Pax6 knockout mice do not show complete loss of β-cells [Sander et al., 1997; Murtaugh, 2006]. It is therefore considered to regulate maturation of β-cells rather than determination of the cell fate. The results of the present study are consistent with those aspects of Pax6. Indeed, AR42J cells could differentiate into insulin-producing cells independent of the presence of Pax6 [Zhang et al., 2001]. Collectively, the functions of Pax6 in basement membrane-mediated differentiation may be mainly due to promotion of maturation rather than determination of the cell fate. It is unclear which signals induce the expression of Pax6 and how Pax6 promotes β-cell differentiation.

We have also found that integrin-activated signal transduction pathways are responsible for the regulation of differentiation induced the by the basement membrane. Specific antibody against

β1-intengrin abrogated upregulation of insulin and Pax6 induced by Matrigel and laminin-1. Particularly, the effect of laminin-1 is almost completely abolished by the treatment with blocking antibody. Note that anti-β1 integrin blocking antibody did not affect differentiation in cells cultured on control dish. This indicates that differentiation of AR42J cells itself occurred independently of β1-integrin signaling. Alternatively, it also possible that AR 42J cells do not produce effective ECMs binding to β1 integrin enough to promote differentiation. Consistent with this hypothesis, we confirmed only low levels of laminin expression in AR42J cells (data not shown). These lines of evidence support the importance of exogenous supplementation of basement membrane for appropriate β-cell differentiation in vitro. Our data agree with the previous study showing that reduction of insulin expression in neonatal islet cells in which β1-integrin interaction is abrogated by gene silencing and the treatment with the blocking antibody [Yashpal et al., 2008]. Our results also extend by showing the role of β1 integrin in regulating the expression of transcription factors.

We also demonstrated the involvement of p38 during differentiation. We found relatively high amounts of phosphorylated p38 in cells cultured on Matrigel and they were abrogated by blocking antibody against β1-integrin (Fig. 6A,B). This indicates that p38 is in downstream of the β1-integrin signaling. These crosstalks of growth factor and β1-integrin signaling in modulating stress kinases are demonstrated by several studies [Mainiero et al., 2000; Bhowmic et al., 2001]. Given that overexpression of transforming growth factor-β-activated kinase 1, an upstream regulator of p38, promotes endocrine differentiation [Ogihara et al., 2003], we postulate that p38 activation is involved in basement membrane-induced differentiation. Interestingly, activation of p38 enhances transcriptional activities of Pax6 through the phosphorylation of its transactivation domain [Mikkola et al., 1999]. Also, β1-integrin-dependent induction of Pax6 during lens development is demonstrated in mice with lens-specific ablation of β1-integrin [Simirskii et al., 2007]. These molecules may modify the function of Pax6, which contributes to promotion of β-cell differentiation induced by the basement membrane. Further studies are needed to clarify the downstream signals of integrin receptor that control regulatory network of the transcriptional factors.

Our findings provide a new insight into the understanding of the role of ECMs in β-cell differentiation. Several lines of evidence indicate that signals from ECM contribute to improved β-cell functions including insulin secretion, glucose responsiveness, and survival [Wang et al., 2005; Parnaud et al., 2006; Pinkse et al., 2006]. However, most of these studies focus on the contribution of ECM to the maintenance of cell functions in isolated β-cells. Our data demonstrate an additional role of the basement membrane as a modulator of β-cell differentiation, and Pax6 is involved in this action. These findings may be helpful to establish cell replacement therapy for diabetes using precursor cells. For instance, when the pancreatic precursor cells are used for the source of β-cell transplantation, the use of basement membrane may promote differentiation to β-cells. Our approach using natural agents is safer than virus-based methods which are well-used to obtain insulin-producing cells. Positive roles of ECMs in β-cell differentiation have been reported in ES cells [Schroeder et al., 2006].

In summary, basement membrane promoted differentiation of AR42J and ductal cells into insulin-producing cells. This effect may be exerted through upregulation of Pax6. These findings provide a new insight into our understanding of the mechanisms for ECM-mediated β-cell differentiation.

REFERENCES

Ahlgren U, Pfaff SL, Jessell TM, Edlund T, Edlund H. 1997. Independent requirement for ISL1 in formation of pancreatic mesenchyme and islet cells. Nature 385:257–260.

Artner I, Blanchi B, Raum JC, Guo M, Kaneko T, Cordes S, Sieweke M, Stein R. 2007. MafB is required for islet beta cell maturation. Proc Natl Acad Sci USA 104:3853–3858.

Ashery-Padan R, Zhou T, Marquardt X, Herrera P, Toube L, Berry A, Gruss P. 2001. Conditional inactivation of Pax6 in the pancreas causes early onset of diabetes. Dev Biol 269:479–488.

Bhowmic NA, Zent R, Ghiassi M, McDonnell M, Moses HL. 2001. Integrin beta 1 signaling is necessary for transforming growth factor-beta activation of p38MAPK and epithelial plasticity. J Biol Chem 276:46707–46713.

Bonner-Weir S, Weir GC. 2005. New sources of pancreatic beta-cells. Nat Biotechnol 23:857–861.

Bonner-Weir S, Taneja M, Weir GC, Tatarkiewicz K, Song KH, Sharma A, O'Neil JJ. 2000. In vitro cultivation of human islets from expanded ductal tissue. Proc Natl Acad Sci USA 97:7999–8004.

Cissell MA, Zhao L, Sussel L, Henderson E, Stein R. 2003. Transcription factor occupancy of the insulin gene in vivo. Evidence for direct regulation by Nkx2.2. J Biol Chem 278:751–756.

Furukawa M, Zhang YQ, Nie L, Shibata H, Kojima I. 1999. Role of mitogen-activated protein kinase and phosphoinositide 3-kinase in the differentiation of rat pancreatic AR42J cells induced by hepatocyte growth factor. Diabetologia 42:450–456.

Harrison KA, Thaler J, Pfaff SL, Gu H, Kehrl JH. 1995. Pancreas dorsal lobe agenesis and abnormal islets of Langerhans in Hlxb9-deficient mice. Nat Genet 23:71–75.

Hynes RO. 2002. Integrins: Bidirectional, allosteric signaling machines. Cell 110:673–687.

Jiang FX, Cram DS, DeAizpurua HL, Harrison LC. 1999. Laminin-1 promotes differentiation of fetal mouse pancreatic beta-cells. Diabetes 48:722–730.

Jiang FX, Naselli G, Harrison LC. 2002. Distinct distribution of laminin and its integrin receptors in the pancreas. J Histochem Cytochem 50:1625–1632.

Jonsson J, Carlsson L, Edlund T, Edlund H. 1994. Insulin-promoter-factor 1 is required for pancreas development in mice. Nature 371:606–609.

Kitamura R, Ogata T, Tanaka Y, Motoyoshi K, Seno M, Takei I, Umezawa K, Kojima I. 2007. Conophylline and betacellulin-delta4: An effective combination of differentiation factors for pancreatic beta cells. Endocr J 54:255–264.

Kren A, Baeriswyl V, Lehembre F, Wunderlin C, Strittmatter K, Antoniadis H, Fässler R, Cavallaro U, Christofori G. 2007. Increased tumor cell dissemination and cellular senescence in the absence of beta1-integrin function. EMBO J 26:2832–2842.

Lammert E, Cleaver O, Melton D. 2001. Induction of pancreatic differentiation by signals from blood vessels. Science 294:564–567.

Li H, Arber S, Jessell TM, Edlund H. 1999. Selective agenesis of the dorsal pancreas in mice lacking homeobox gene Hlxb9. Nat Genet 23:67–70.

Mainiero F, Soriani A, Strippoli R, Jacobelli J, Gismondi A, Piccoli M, Frati L, Santoni A. 2000. RAC1/P38 MAPK signa ling pathway controls beta1 integrin-induced interleukin-8 production in human natural killer cells. Immunity 12:7–16.

Mashima H, Ohnishi H, Wakabayashi K, Mine T, Miyagawa J, Hanafusa T, Seno M, Yamada H, Kojima I. 1996. Betacellulin and activin A coordinately convert amylase-secreting pancreatic AR42J cells into insulin-secreting cells. J Clin Invest 97:1647–1654.

Mashima H, Yamada S, Tajima T, Seno M, Yamada H, Takeda J, Kojima I. 1999. Genes expressed during differentiation of pancreatic AR42J cells to insulin-secreting cells. Diabetes 48:304–309.

Mikkola I, Bruun JA, Bjorkoy G, Holm T, Johansen T. 1999. Phosphorylation of the transactivation domain of Pax6 by extracellular signal-regulated kinase and p38 mitogen-activated protein kinase. J Biol Chem 274: 15115–15126.

Murtaugh LC. 2006. Pancreas and beta-cell development: From the actual to the possible. Development 134:427–438.

Naya FJ, Huang HP, Qiu Y, Mutoh H, DeMay AB, Leiter Tsai MJ. 1997. Diabetes, defective pancreatic morphogenesis, and abnormal enteroendocrine differentiation in BETA2/neuroD-deficient mice. Genes Dev 11:2323–2334.

Nikolova G, Jabs N, Konstantinova I, Domogatskaya A, Tryggvason K, Sorokin L, Fässler R, Gu G, Gerber HP, Ferrara N, Melton DA, Lammert E. . The vascular basement membrane: A niche for insulin gene expression and Beta cell proliferation. Dev Cell 10:397–405.

Offield MF, Jetton TL, Labosky PA, Ray M, Stein RW, Magnuson MA, Hogan BL, Wright CV. 1996. PDX-1 is required for pancreatic outgrowth and differentiation of the rostral duodenum. Development 122:983–995.

Ogata T, Li K, Seno M, Kojima I. 2004. Reversal of streptozotocin-induced diabetes by transplantation of β cells derived from ductal cells. Endocr J 51:381–386.

Ogihara T, Watada H, Kanno R, Ikeda F, Nomiyama T, Tanaka Y, Nakao A, German MS, Kojima I, Kawamori R. 2003. p38 MAPK is involved in activin A- and hepatocyte growth factor-mediated expression of pro-endocrine gene neurogenin 3 in AR42J-B13 cells. J Biol Chem 278:21693–21700.

Ohnishi H, Ohgushi N, Tanaka S, Mogami H, Nobusawa R, Mashima H, Furukawa M, Mine T, Shimada O, Ishikawa H, Kojima I. 1995. Conversion of amylase-secreting rat pancreatic AR42J cells to neuronlike cells by activin. J Clin Invest 95:2304–2314.

Olbrot M, Rud J, Moss LG, Sharma A. 2002. Identification of beta-cell-specific insulin gene transcription factor RIPE3b1 as mammalian MafA. Proc Natl Acad Sci USA 99:6737–6742.

Parnaud G, Hammar E, Rouiller DG, Armanet M, Halban PA, Bosco D. 2006. Blockade of beta1 integrin-laminin-5 interaction affects spreading and insulin secretion of rat beta-cells attached on extracellular matrix. Diabetes 55:1413–1420.

Pinkse GG, Bouwman WP, Jiawan-Lalai R, Terpstra OT, Bruijn JA, de Heer E. 2006. Integrin signaling via RGD peptides and anti-beta1 antibodies confers resistance to apoptosis in islets of Langerhans. Diabetes 55:312–317.

Riquelme C, Larrain J, Schonherr E, Henriquez JP, Kresse H, Brandan E. 2001. Antisense inhibition of decorin expression in myoblasts decreases cell responsiveness to transforming growth factor beta and accelerates skeletal muscle differentiation. J Biol Chem 276:3589–3596.

Sander M, Neubüser A, Kalamaras J, Ee HC, Martin GR, German MS. 1997. Genetic analysis reveals that PAX6 is required for normal transcription of pancreatic hormone genes and islet development. Genes Dev 11:1662–1673.

Sander M, Sussel L, Conners J, Scheel D, Kalamaras J, Dela Cruz F, Schwitzgebel V, Hayes-Jordan A, German M. 2000. Homeobox gene Nkx6.1 lies downstream of Nkx2.2 in the major pathway of beta-cell formation in the pancreas. Development 127:5533–5540.

Schroeder IS, Rolletschek A, Blyszczuk P, Kania G, Wobus AM. 2006. Differentiation of mouse embryonic stem cells to insulin-producing cells. Nat Protoc 1:495–507.

Seno M, Tada H, Kosaka M, Sasada R, Igarashi K, Shing Y, Folkman J, Ueda M, Yamada H. 1996. Human betacellulin, a member of the EGF family dominantly expressed in pancreas and small intestine, is fully active in a monomeric form. Growth Factors 13:181–191.

Simirskii VN, Wang Y, Duncan MK. 2007. Conditional deletion of beta1-integrin from the developing lens leads to loss of the lens epithelial phenotype. Dev Biol 306:658–668.

Sosa-Pineda B, Chowdhury K, Torres M, Oliver G, Gruss P. 1997. The Pax4 gene is essential for differentiation of insulin-producing beta cells in the mammalian pancreas. Nature 386:399–402.

St-Onge L, Sosa-Pineda B, Chowdhury K, Mansouri A, Gruss P. 1997. Pax6 is required for differentiation of glucagon-producing alpha-cells in mouse pancreas. Nature 387:406–409.

Sussel L, Kalamaras L, Hartigan-O'Connor DL, Meneses JJ, Pedersen RA, Rubenstein JL, German MS. 1998. Mice lacking the homeodomain transcription factor Nkx2.2 have diabetes due to arrested differentiation of pancreatic beta cells. Development 125:2213–2221.

Suzuki A, Iwama A, Miyashita H, Nakauchi H, Taniguchi H. 2003. Role for growth factors and extracellular matrix in controlling differentiation of prospectively isolated hepatic stem cells. Development 130:2513–2524.

Wang R, Li J, Lyte K, Yashpal NK, Fellows F, Goodyer CG. 2005. Role for beta1 integrin and its associated alpha3, alpha5, and alpha6 subunits in development of the human fetal pancreas. Diabetes 54:2080–2089.

Yamaoka T, Yano M, Yamada T, Matsushita T, Moritani M, Ii S, Yoshimoto K, Hata J, Itakura M. 2000. Diabetes and pancreatic tumours in transgenic mice expressing Pax 6. Diabetologia 43:332–339.

Yashpal NK, Li J, Wheeler MB, Wang R. 2008. Expression of {beta}1 integrin receptors during rat pancreas development—Sites and dynamics. Endocrinology 146:1798–1807.

Yoshitomi H, Zaret KS. 2004. Endothelial cell interactions initiate dorsal pancreas development by selectively inducing the transcription factor Ptf1a. Development 131:807–817.

Zhang YQ, Mashima H, Kojima I. 2001. Changes in the expression of transcription factors in pancreatic AR42J cells during differentiation into insulin-producing cells. Diabetes 50 (Suppl 1):S10–S14.

ISSN 0026-8933, Molecular Biology, 2012, Vol. 46, No. 1, pp. 142–148. © Pleiades Publishing, Inc., 2012.

STRUCTURAL AND FUNCTIONAL ANALYSIS OF BIOPOLYMERS AND THEIR COMPLEXES

UDC 577.772 072

The Conformational Polymorphism of the Green Fluorescent Protein[1]

Haidong Tan[a], Yueguang Li[b], Ling Chen[c], Takayuki Kudoh[c], Tomonari Kasai[c], and Masaharu Seno[c]

[a] *Dalian Institute of Chemical Physics, CAS, Dalian 116023, China*

[b] *Department of General Surgery, Tianjin 4th Centre Hospital, Zhongshanlu, Hebeiqu, Tianjin 300140, People's Republic of China*

[c] *Department of Medical and Bioengineering Science, Graduate School of Natural Science and Technology, Okayama University, Okayama 700-8530, Japan;*

e-mail: mseno@cc.okayama-u.ac.jp

Received November 9, 2010; in final form, January 13, 2011

Abstract—Green fluorescent protein (GFPuv) has been widely used as a reporter fused to individual targeting sequences. However, its state in liquid and its effect on other proteins are still unclear. The conformational polymorphisms of glutathione-S-transferase-green fluorescent protein (GST-GFPuv), GFPuv and GST were analyzed by native polyacrylamide gel, indicating that GST was in many different states while GFPuv and GST-GFPuv were only in four and two slightly different states. Four different circular dichroism spectra were obtained from the GFPuv polymorphisms. The single molecular behavior of GST-GFPuv and GFPuv was also characterized by MALDI-TOF MS. Thus, we demonstrated that: (1) there might be four different structural polymorphisms for the native GFPuv; (2) GFPuv could reduce its partner's polymorphism as a fusion protein. Although GFPuv had many merits as a reporter, its unreliability was found in the study.

DOI: 10.1134/S0026893311060045

Keywords: green fluorescent protein, conformational polymorphism, glutathione-S-transferase, native polyacrylamide gel electrophoresis, MALDI-TOF MS, circular dichroism spectra

Although crystal structures of many proteins have been extensively provided [1, 2], the exact structures of the proteins in their native states are still poorly understood [3]. Thus, the structural polymorphisms of native proteins are the basic information for understanding their exact structure.

The green fluorescent protein (GFPuv) is exceptionally widely utilized in cell biology as a natural, brightly fluorescent marker for gene expression, localization of gene products and intracellular protein to protein interactions [4–8]. In order to understand the complex photo physics of GFPuv, a considerable number of studies has been published [9–12]. Thus, GFPuv can be a potential candidate to help us to understand such polymorphisms. The crystal structure of GFPuv is a cylinder, which ensures stable positioning [13] and makes the protein very stable even under strict conditions [14, 15].

In liquid, the secondary structure of proteins can be determined by CD spectroscopy in the far-UV spectral region (190–250 nm). Thus, the method has been widely used for measuring the structure of GFPuv in its native state [16, 17]. However, the structure of GFPuv is a cylinder with two flexible loops at the two ends, so the structure might have more than only one conformation in its native state. The present study is directed towards investigation of the structural polymorphisms of GFPuv and its effects on its' partner in a fusion protein.

On the other hand, GFPuv has been widely used as a reporter fused to individual targeting sequences in the articles, published in most of the leading journals, including *Cell*, *Science* and *Nature*. However, the routine lab method's accuracy may be called into question because GFPuv may affect its partner's function and location in the cell [18, 19]. Also, a strong constant signal from the GFPuv may remain even when its partner is degraded, because GFPuv is highly resistant to protease degradation [20] and can be fused to ubiquitin during the expression [21, 22]. Here, this problem was also found.

EXPERIMENTAL

Materials. Expression vector pET41a was purchased from Novagen (USA). Modified pEGFP-1 plasmid (Avoiding restriction digestion site existed in the GFPuv gene, site-directed mutagenesis was used to change the corresponding sites as A178G site and C423G site) was kindly supplied by Zongbao Zhao.

[1] The article is published in the original.

Escherichia coli BL21 (DE3) and *E. coli* DH5α, plasmid mini-preparation kit, high fidelity polymerase and other reagents were purchased from Dingguo Biotech (China). Standard EK was purchased from New England BioLabs Ltd (China). Primers, restriction enzymes and the T4 DNA ligase were from TaKaRa Biotechnology (China).

Plasmid construction. The GFPuv gene was amplified using a modified pEGFP-1 plasmid as template by PCR with a forward primer 5'-GCGGAATTCAGTAAAGGAGAAGAAC-3' and, a reverse primer 5'-CGGATCCTCGAGTTATTTGTAGAGCTC-3'. The PCR was performed according to the following thermocycle: an initial denaturing step at 95°C for 2 min, 30 cycles (95°C for 30 s, 58°C for 30 s, 72°C for 1 min), and additional extension at 72°C for 10 min. The PCR product was cleaved by *Eco*RI and *Xho*I and cloned into the corresponding sites in pET41a to obtain the expression plasmid pET41a-GFPuv and then transformed into *E. coli* BL21 (DE3).

Fusion protein expression and purification. One colony of *E. coli* BL21(DE3) containing pET41a-GFPuv plasmids was picked and transferred into 25 mL LB medium containing kanamycin (50 μg/mL) and cultured at 200 rpm shaking at 37°C overnight. 10 mL culture was added to 1 l of LB broth containing kanamycin (50 μg/mL) and 0.1 mM IPTG and incubated at 37°C for 10 h.

All of the cells were harvested by centrifugation at 5000 *g* for 15 min and washed twice with 500 mM NaCl, 20 mM Tris-HCl, pH 8.0 buffer. Finally, ultrasonic methods were used to disrupt the host strain. The disrupted cell liquid was centrifuged at 12000 *g* for 15 min, and the supernatants were collected, added 70 mM imidazole and loaded onto a Ni-NTA column, pre-equilibrated with the same buffer and the same concentration of imidazole, for purification. The proteins were eluted from the column by 250 mM imidazole, 20 mM sodium phosphate and 500 mM NaCl.

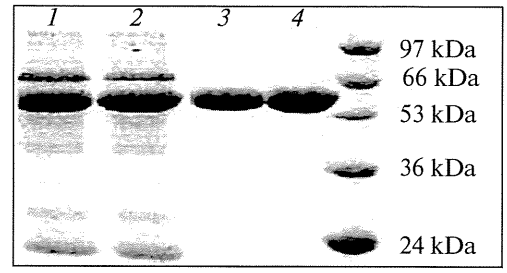

Fig. 1. SDS-PAGE analysis of GST-GFPuv purification using Ni-NTA purification system. Lanes *1* and *2*„ Unpurified GST-GFPuv. Lanes *3* and *4*„ GST-GFPuv purified through two steps (loading buffer with 70 mM imidazole and eluting liquid with 250 mM imidazole).

The fusion protein glutathione-S-transferase-green fluorescent protein (GST-GFPuv), harboring an enterokinase site between GST and GFPuv, was purified.

Conformational polymorphism analysis by native polyacrylamide gel electrophoresis (PAGE). Initially the purified proteins were dialyzed against the buffer (2 mM $CaCl_2$, 100 mM NaCl and 20 mM Tris-HCl, pH 8.0) at 4°C for 24 h. 50 μg GST-GFPuv were cleaved by 2 u enterokinase at 25°C for 24 h. GFPuv with a His-tag at the C terminus was further purified using the above mentioned Ni-NTA purification system. All of the samples were analyzed by native PAGE [23]. Using UV lamps (300 nm) as an illumination source, the conformational polymorphisms of GST-GFPuv and GFPuv were determined by native PAGE since the proteins were separated according to the net charge, size and shape of their native structures. For direct visualization of the proteins, the gel was stained with Coomassie Brilliant Blue R-250.

Circular dichroism measurements. The four bands of the cleaved GFPuv (Fig. 2) on the SDS-PAGE gel were excised respectively and washed in a solution

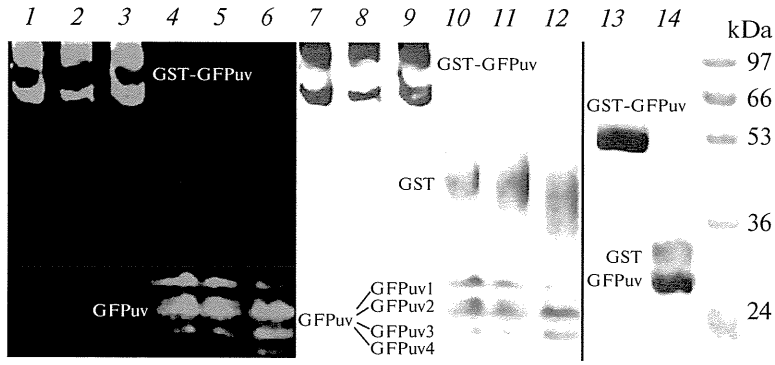

Fig. 2. Native PAGE analysis of purified GST-GFPuv, GST and GFPuv (lanes *1–12*). To separate the native proteins we used 5% stacking gel and 12% separating gel. GST and GFPuv were released when GST-GFPuv was cleaved by enterokinase. For comparison, the gel was also visualized with Coomassie Brilliant Blue R-250 staining. Lanes *13–14*„ SDS-PAGE analysis of the molecular weight of GST-GFPuv, GST and GFPuv. For comparison, the samples were also visualized with Coomassie Brilliant Blue R-250 staining.

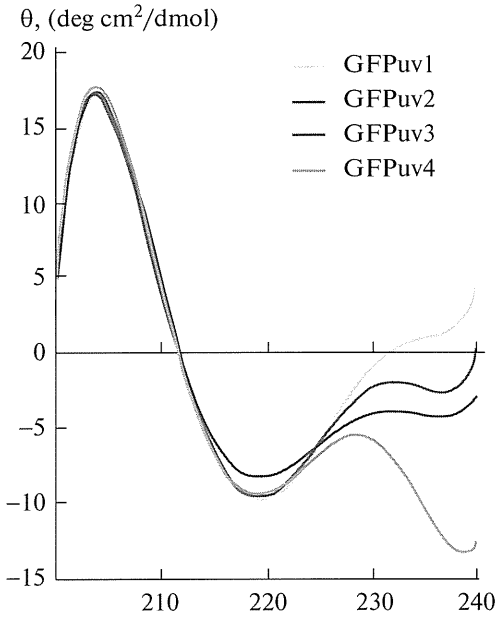

Fig. 3. Experimental far-UV CD spectra of GFPuv at pH 7.5. The secondary structure content recovered by the CONTIN program was as follows: α-helix 20%, β-sheet 48%, β-turn 14% and the remainder 18%. The results are based on three different experiments, in which the recovered values were averaged. GFPuv1, GFPuv2, GFPuv3 and GFPuv4 were consistent with those in Fig. 3.

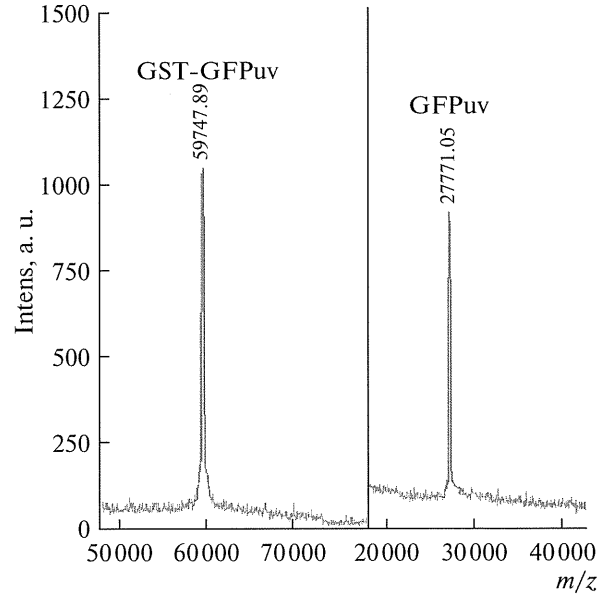

Fig. 4. MALDI-TOF MS analysis of purified GST-GFPuv and GFPuv. The purified GST-GFPuv appeared as two states on the native PAGE while the purified GFPuv appeared as four states on the PAGE (Fig. 3). One microliter of the GST-GFPuv or GFPuv was desalted through a C18 ZipTip (Millipore). The ZipTip was activated, equilibrated, and loaded according to the manufacturer's instructions. The bound material was then eluted with α-cyano-4-hydroxycinnamic acid (10 mg/ml) in 70% acetonitrile containing 0.1% TFA before being spotted and co-crystallized.

containing 100 mM potassium phosphate (pH 8.0), 50 mM NaCl, and 1 mM EDTA. CD wavelength scans were recorded with a Jasco J-715 spectropolarimeter (Jasco, Japan). The protein samples were prepared with a concentration of 0.1 mg mL^{-1}. All spectra were recorded at 25°C with 10 scans. The data was normalized to a molar ellipticity with a path length of 0.1 cm.

MALDI-TOF MS analysis of GST-GFPuv and GFPuv. To avoid the mutants of GST-GFPuv and GFPuv causing the polymorphism of the molecules, MALDI-TOF MS analysis of GST-GFPuv and purified GFPuv were performed. The experimental protocol for sample preparation and MALDI analysis was described elsewhere [24]. The samples were analyzed on a MALDI-TOF mass spectrometer (Bruker Autof-

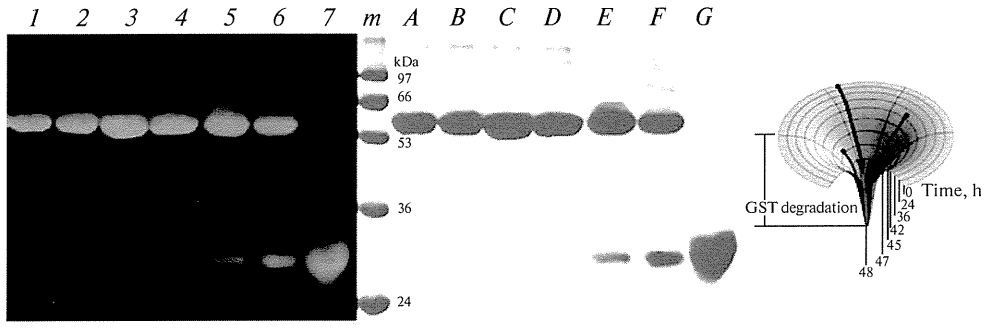

Fig. 5. Detection of GST-GFPuv degradation in SDS-PAGE. GST-GFPuv was incubated at 37°C for 0, 24, 36, 42, 45, 47 and 48 h (lanes *1*–*7*). For comparison, the gel was also stained with Coomassie Brilliant Blue R250 (lanes *A*–*G*). GST degradation is shown as a cartoon model to the right. From 0 to 42 h, the degradation was too low to be detected but the conformation would change slightly preparing for degradation. When the change accumulated to a certain degree, degradation would be promoted abruptly after 42 h of incubation.

lex, Bruker-Daltonics, Germany). Mass calibration was performed with aqueous solutions of lysine, trehalose and alanine. The accuracy was ±0.1 apparent mass units.

Unreliability for GFPuv as a reporter. GST-GFPuv was incubated at 37°C for 0, 24, 36, 42, 45, 47 and 48 h, respectively. The samples were detected by SDS-PAGE using UV lamps (300 nm) as an illumination source. For direct visualization of the proteins, the gel was stained with Coomassie Brilliant Blue R-250. The molecular weight of the samples was determined by SDS-PAGE.

RESULTS AND DISCUSSION

Amplification of the GFPuv Gene and Plasmid Construction

The GFPuv gene was amplified by PCR using a modified pEGFP-1 plasmid as a template. A DNA fragment of about 0.7 kb was obtained, what coincided with the expected fragment length. The PCR product was purified and digested with *Eco*RI/*Xho*I, and cloned into plasmid pET-41a between the *Eco*RI/*Xho*I restriction sites downstream of the fusion partner GST to give pET41a-GFPuv.

Fusion Protein Expression and Purification

Upon induction with IPTG, the fusion protein could be highly expressed (500 mg GST-FPuv L^{-1}). Illuminating the Ni-NTA affinity column with a long UV lamp ($\lambda = 365$ nm), protein purification could be clearly tracked and optimized. Thus highly purified GST-GFPuv was obtained without a washing step (Fig. 1).

The Conformational Polymorphism of GFPuv

The structural polymorphisms of GST-GFPuv and GFPuv (the latter was obtained by digesting the fusion protein with an enterokinase) were observed by native PAGE using UV lamps (300 nm) as an illumination source. As Fig. 2 showed, GST was in a smear, while GFPuv and GST-GFPuv were in four and two slightly different states, respectively. The slight difference of GFPuv or GST-GFPuv should be caused by the structural polymorphisms since the proteins were separated according to the net charge, size and shape of their native structures.

Unlike the mess of polymorphisms of GST observed in its free state in the fusion protein only two states of GST were present (Fig. 2), suggesting that GFPuv could reduce the number of its partner's conformational polymorphisms. Thus, GFPuv was very useful to avoid hydrophobic interactions and improve the refolding of its partner during recombinant protein expression. GST was also fused to other proteins but was often presented as a mess on the native gel [23].

In native PAGE proteins are separated according to the net charge, size and shape of their native structure. According to the protocol mentioned in the previous report [25], the relation between electrophoresis velocity and protein compact degree was established as: $V = \frac{P\sqrt{-Q}}{CDM}$, where V stands for electrophoresis velocity (cm h^{-1}), P stands for power (watt), Q—protein charge, C—protein compact degree, D stands for the percentage of the gel and M—for the molecular weight of the protein (Dalton). The structural polymorphism of protein is mainly caused by the parameter C. In our results, the C values were almost the same for GST-GFPuv and GFPuv, but quite different from the value of GST. Thus, we suggested that GFPuv has a mooring function and reduces the number of its partner's polymorphisms.

Circular Dichroism Measurements

The four single protein bands on the SDS-PAGE gel were analyzed by Jasco J-715 spectropolarimeter. They show four different circular dichroism spectra, in which the α-helix, β-sheet and β-turn were almost the same, while the remainder was different (Fig. 3). We guess that the remainder might be the side loops on the both ends, which are flexible and may cause the different structural polymorphisms in GFPuv (Fig. 2). Other structures, such as the α-helix, β-sheet and β-turn, were very stable, forming a cylinder with a rigid structure. Our results were different from previous reports [16, 17], in which only one native structure was reported.

MALDI-TOF MS Analysis of GST-GFPuv and GFPuv

To avoid the polymorphism caused by the mutants of GST-GFPuv and GFPuv, MALDI-TOF MS analysis was performed. The single molecular behavior of GST-GFPuv and GFPuv was characterized by MALDI-TOF MS although they appeared as two states and four states in native PAGE (Figs. 2 and 4). The molecular weights of GST-GFPuv and GFPuv were consistent with their theoretical values (Fig. 4), so there were no mutants among the molecules. Thus, these results further proved that the different polymorphisms might be caused by different conformations, but not by the mutants. For GST, there were many polymorphisms, which were hard to analyze by CD spectra. However, the polymorphisms could be reduced by its partner in the fusion protein (Fig. 2).

Unreliability of GFPuv as a Reporter

GFPuv has been widely used as a reporter fused to individual targeting sequences (table). However, the accuracy of routine lab methods may be called into

Previous reports for GFPuv's partners and possible mechanisms of the fusion protein degradation

GFPuv's partner used in the publications of *Cell*, *Nature*, and *Science*	Possible degradation mechanism
P450 (*1*, *2*)	Ubiquitin-dependent proteasomal degradation (*3–22*)
Arginine vasopressin (*23*)	Vasopressinase (*24-29*)
Alkaline phosphatase (*30*)	Ubiquitin-dependent proteasomal degradation (*31–33*)
Leptin (*34*)	Ubiquitin-dependent proteasomal degradation (*35–37*)
Actin (*38*, *39*)	Ubiquitin-dependent proteasomal degradation (*40–52*)
Myc (*53*)	Ubiquitin-dependent proteasomal degradation (*54–78*)
c-kit (*79*)	Ubiquitin-dependent proteasomal degradation (*80–83*)
Raf (*84*)	Ubiquitin-dependent proteasomal degradation (*85–90*)
CLIP170 (*91*)	Ubiquitin-dependent proteasomal degradation (*92*)
GluR-A (*93*)	Ubiquitin-dependent proteasomal degradation (*94–96*)
Nras/Kras4B (*97*)	Ubiquitin-dependent proteasomal degradation (*98–100*)
VSVG (*101*)	VSV acid-activation (*102–105*)
Calmodulin (*106*)	20S proteasome (*107–111*)
Integrin (*112*)	Ubiquitin-dependent proteasomal degradation (*113–116*)
Glucocorticoid receptor (*117*)	Ubiquitin-dependent proteasomal degradation (*118–125*)
ErbB1 (*126*)	c-Cbl-regulation (*127–130*)
Histone H1 (*131*)	Ubiquitin-dependent proteasomal degradation (*132–135*)
Dynamin (*136*)	Ubiquitin-dependent proteasomal degradation (*137–140*)
Myosin II (*141*)	Ubiquitin-dependent proteasomal degradation (*142–144*)
VEGF (*145*)	Ubiquitin-dependent proteasomal degradation (*146–148*)

Note: GFPuv is highly resistant to protease degradation (*149*) and can be fused to ubiquitin during expression (*150*, *151*). The number stands for the corresponding references, all of which can be viewed in supplementary material (please contact with corresponding author).

question because GFPuv is highly stable and resistant to protease degradation, heat and chemical denaturation, while many of its partners may be unstable and easily proteolyzed (table). Here, GFPuv's unreliability was also found. Its partner was degraded after 42 h of incubation at 37°C, but a strong fluorescent signal remained constant (Fig. 5). However, this seemed very unreasonable, because it would be expected that the degradation would have occured during the entire period. We guess that the degradation is too low to be detected at the beginning, and the conformation will change slightly preparing for degradation. When the changes accumulate to a certain degree, degradation can be promoted abruptly (Fig. 5). Meanwhile, mass spectrum analysis revealed that there were still eight amino acid residues located upstream of the GFPuv after fusion protein degradation.

Frankly, the stability of GFPuv is not absolute. GFPuv was stable, but could be destabilized by the addition of putative proteolytic signal sequences [26]. Additionally, a destabilized GFP could be created by fusing amino acids 422–461 of the degradation domain of mouse ornithine decarboxylase (MODC) to the C-terminal end of GFPuv. The fusion protein was unstable in the presence of cycloheximide and had a fluorescence half-life of 2 h [27]. In the same way, the fusion protein GFPuv-IkB can be degraded as well as IkB upon TNFa treatment [28]. Likely, short-lived

green fluorescent proteins could also be created by fusing with ubiquitin [29]. Therefore, on the contrary, if some proteins were more stable than GFPuv and GFPuv would be degraded in a short time, the target protein would still exist although the signal would be gone.

Thus, to improve standardization, the intactness of its partner should be checked if GFPuv was used as a reporter. Sometimes western blotting may be essential.

CONCLUSIONS

There might be four slightly different structural polymorphisms for the native GFPuv. Thus, it is a potential candidate to explore the exact structure of the native protein. Because of its polymorphism, GFPuv could reduce its partner's polymorphisms in a fusion protein. Although GFPuv has many merits as a reporter, its unreliability should be considered in many fields of research.

ACKNOWLEDGMENTS

We appreciate Ms. Mami Asakura for her excellent technical assistance. We also thank the anonymous reviewer for his or her insightful suggestions.

The financial support of the National Basic Research Program of China (973 Program) (no. 2007CB707802) is gratefully acknowledged.

REFERENCES

1. May P., Kreuchwig A., Steinke T., Koch I. 2010. PTGL: A database for secondary structure-based protein topologies. *Nucleic Acids Res.* **38**, D326–D330.
2. Lobanov M., Bogatyreva N.S., Ivankov D.N., Finkel'shtein A.V. 2009. Protein structure prediction from analogy: 1. New database of spatially similar and dissimilar structures of protein domains for testing and optimization of prediction methods. *Mol. Biol.* (Moscow). **43**, 722–732.
3. Eyal E., Gerzon S., Potapov V., Edelman M., Sobolev V. 2005. The limit of accuracy of protein modeling: Influence of crystal packing on protein structure. *J. Mol. Biol.* **351**, 431–442.
4. Leclercq J., Lardet L., Martin F., Chapuset T., Oliver G., Montoro P. 2010. The green fluorescent protein as an efficient selection marker for *Agrobacterium tumefaciens*-mediated transformation in *Hevea brasiliensis* (Mull. Arg). *Plant Cell Rep.* **29**, 513–522.
5. Zhang Z., Dharmakumar R., Mascheri N., Fan Z., Wu S., Li D. 2009. Comparison of superparamagnetic and ultrasmall superparamagnetic iron oxide cell labeling for tracking green fluorescent protein gene marker with negative and positive contrast magnetic resonance imaging. *Mol. Imaging.* **8**, 148–155.
6. Li W., Zhang N., Liang X., Li J., Gong P., Yu X., Ma G., Ryan U.M., Zhang X. 2009. Transient transfection of *Cryptosporidium parvum* using green fluorescent protein (GFP) as a marker. *Mol. Biochem. Parasitol.* **168**, 143–148.
7. Kim H.S., Cho H.R., Choi S.H., Woo J.S., Moon W.K. 2010. *In vivo* imaging of tumor transduced with bimodal lentiviral vector encoding human ferritin and green fluorescent protein on a 1.5T clinical magnetic resonance scanner. *Cancer Res.* **70**, 7315–7324.
8. Viczian A., Kircher S. 2010. Luciferase and green fluorescent protein reporter genes as tools to determine protein abundance and intracellular dynamics. *Methods Mol. Biol.* **655**, 293–312.
9. Garcia-Parajo M.F., Segers-Nolten G.M., Veerman J.A., Greve J., van Hulst N.F. 2000. Real-time light-driven dynamics of the fluorescence emission in single green fluorescent protein molecules. *Proc. Natl. Acad. Sci. U.S.A.* **97**, 7237–7242.
10. Kubitscheck U., Kuckmann O., Kues T., Peters R. 2000. Imaging and tracking of single GFP molecules in solution. *Biophys. J.* **78**, 2170–2179.
11. Haupts U., Maiti S., Schwille P., Webb W.W. 1998. Dynamics of fluorescence fluctuations in green fluorescent protein observed by fluorescence correlation spectroscopy. *Proc. Natl. Acad. Sci. U.S.A.* **95**, 13573–13578.
12. Creemers T.M., Lock A.J., Subramaniam V., Jovin T.M., Volker S. 2000. Photophysics and optical switching in green fluorescent protein mutants. *Proc. Natl. Acad. Sci. U.S.A.* **97**, 2974–2978.
13. Yang F., Moss L.G., Phillips G.N., Jr. 1996. The molecular structure of green fluorescent protein. *Nature Biotechnol.* **14**, 1246–1251.
14. Ishii M., Kunimura J.S., Jeng H.T., Penna T.C., Cholewa O. 2007. Evaluation of the pH- and thermal stability of the recombinant green fluorescent protein (GFP) in the presence of sodium chloride. *Appl. Biochem. Biotechnol.* **137–140**, 555–571.
15. Penna T.C., Ishii M., Junior A.P., Cholewa O. 2004. Thermal stability of recombinant green fluorescent protein (GFPuv) at various pH values. *Appl. Biochem. Biotechnol.* **113–116**, 469–483.
16. Iwai H., Lingel A., Pluckthun A. 2001. Cyclic green fluorescent protein produced *in vivo* using an artificially split PI-PfuI intein from *Pyrococcus furiosus*. *J. Biol. Chem.* **276**, 16548–16554.
17. Visser N.V., Hink M.A., Borst J.W., van der Krogt G.N., Visser A.J. 2002. Circular dichroism spectroscopy of fluorescent proteins. *FEBS Lett.* **521**, 31–35.
18. Hanson D.A., Ziegler S.F. 2004. Fusion of green fluorescent protein to the C-terminus of granulysin alters its intracellular localization in comparison to the native molecule. *J. Negat. Results Biomed.* **3**, 2.
19. Prescott M., Nowakowski S., Nagley P., Devenish R.J. 1999. The length of polypeptide linker affects the stability of green fluorescent protein fusion proteins. *Anal. Biochem.* **273**, 305–307.
20. Roucou X., Prescott M., Devenish R.J., Nagley P. 2000. A cytochrome c-GFP fusion is not released from mitochondria into the cytoplasm upon expression of *Bax* in yeast cells. *FEBS Lett.* **471**, 235–239.

21. Perroy J., Pontier S., Charest P.G., Aubry M., Bouvier M. 2004. Real-time monitoring of ubiquitination in living cells by BRET. *Nature Methods*. **1**, 203–208.

22. Dantuma N.P., Groothuis T.A., Salomons F.A., Neefjes J. 2006. A dynamic ubiquitin equilibrium couples proteasomal activity to chromatin remodeling. *J. Cell Biol.* **173**, 19–26.

23. Wang C., Meier U.T. 2004. Architecture and assembly of mammalian H/ACA small nucleolar and telomerase ribonucleoproteins. *EMBO J.* **23**, 1857–1867.

24. Liao C.C., Mehta A., Ward N.J., Marsh S., Arulampalam T., Norton J.D. 2010. Analysis of post-operative changes in serum protein expression profiles from colorectal cancer patients by MALDI-TOF mass spectrometry: A pilot methodological study. *World J. Surg. Oncol.* **8**, 33.

25. Gallagher S. 2001. One-dimensional electrophoresis using nondenaturing conditions. *Curr. Protoc. Protein Sci.* Chapter 10, Unit 10 13.

26. Corish P., Tyler-Smith C. 1999. Attenuation of green fluorescent protein half-life in mammalian cells. *Protein Eng.* **12**, 1035–1040.

27. Li X., Zhao X., Fang Y., Jiang X., Duong T., Fan C., Huang C.C., Kain S.R. 1998. Generation of destabilized green fluorescent protein as a transcription reporter. *J. Biol. Chem.* **273**, 34970–34975.

28. Li X., Fang Y., Zhao X., Jiang X., Duong T., Kain S.R. 1999. Characterization of NFkappaB activation by detection of green fluorescent protein-tagged IkappaB degradation in living cells. *J. Biol. Chem.* **274**, 21244–21250.

29. Dantuma N.P., Lindsten K., Glas R., Jellne M., Masucci M.G. 2000. Short-lived green fluorescent proteins for quantifying ubiquitin/proteasome-dependent proteolysis in living cells. *Nature Biotechnol.* **18**, 538–543.

ACCOUNTS
of chemical research

Efficient Intracellular Delivery of Nucleic Acid Pharmaceuticals Using Cell-Penetrating Peptides

IKUHIKO NAKASE,[†] HIDETAKA AKITA,[‡] KENTARO KOGURE,[§] ASTRID GRÄSLUND,[∥] ÜLO LANGEL,[⊥] HIDEYOSHI HARASHIMA,[‡] AND SHIROH FUTAKI*,[†]

[†]*Institute for Chemical Research, Kyoto University, Uji, Kyoto 611-0011, Japan,* [‡]*Faculty of Pharmaceutical Sciences, Hokkaido University, Sapporo, Hokkaido 060-0812, Japan,* [§]*Department of Biophysical Chemistry, Kyoto Pharmaceutical University, Kyoto, Kyoto 607-8414, Japan,* [∥]*Department of Biochemistry and Biophysics, Arrhenius Laboratories for Natural Sciences, Stockholm University, 10691 Stockholm, Sweden, and* [⊥]*Department of Neurochemistry, Stockholm University, 10692 Stockholm, Sweden*

RECEIVED ON OCTOBER 6, 2011

CONSPECTUS

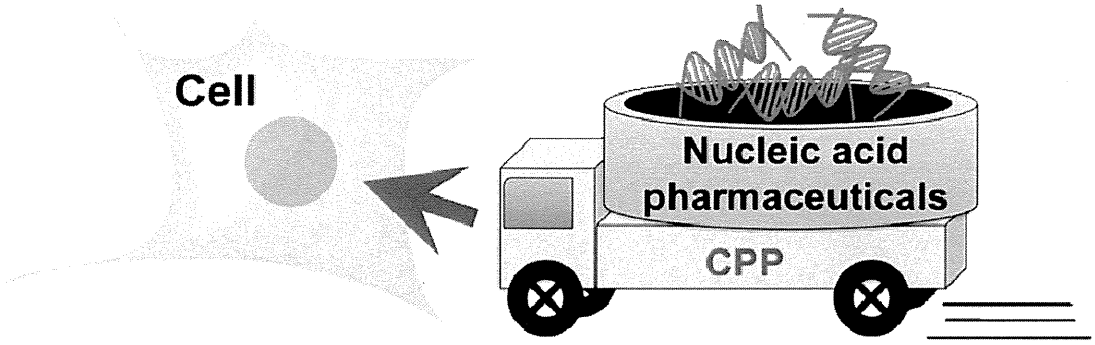

Over the last 20 years, researchers have designed or discovered peptides that can permeate membranes and deliver exogenous molecules inside a cell. These peptides, known as cell-penetrating peptides (CPPs), typically consist of 6−30 residues, including HIV TAT peptide, penetratin, oligoarginine, transportan, and TP10. Through chemical conjugation or noncovalent complex formation, these structures successfully deliver bioactive and membrane-impermeable molecules into cells. CPPs have also gained attention as an attractive vehicle for the delivery of nucleic acid pharmaceuticals (NAPs), including genes/plasmids, short oligonucleotides, and small interference RNAs and their analogues, due to their high internalization efficacy, low cytotoxicity, and flexible structural design.

In this Account, we survey the potential of CPPs for the design and optimization of NAP delivery systems. First, we describe the impact of the N-terminal stearylation of CPPs. Endocytic pathways make a major contribution to the cellular uptake of NAPs. Stearylation at the N-terminus of CPPs with stearyl-octaarginine (R8), stearyl-$(RxR)_4$, and stearyl-TP10 prompts the formation of a self-assembled core−shell nanoparticle with NAPs, a compact structure that promotes cellular uptake. Researchers have designed modifications such as the addition of trifluoromethylquinoline moieties to lysine residues to destabilize endosomes, as exemplified by PepFect 6, and these changes further improve biological responsiveness. Alternatively, stearylation also allows implantation of CPPs onto the surface of liposomes. This feature facilitates "programmed packaging" to establish multifunctional envelope-type nanodevices (MEND). The R8-MEND showed high transfection efficiency comparable to that of adenovirus in non-dividing cells.

Understanding the cellular uptake mechanisms of CPPs will further improve CPP-mediated NAP delivery. The cellular uptake of CPPs and their NAP complex involves various types of endocytosis. Macropinocytosis, a mechanism which is also activated in response to stimuli such as growth factors or viruses, is a primary pathway for arginine-rich CPPs because high cationic charge density promotes this endocytic pathway. The use of larger endosomes (known as macropinosomes) rather than clathrin- or caveolae-mediated endocytosis has been reported in macropinocytosis which would also facilitate the endocytosis of NAP nanoparticles into cells.

www.pubs.acs.org/accounts
10.1021/ar200256e

1. Introduction

Around 20 years ago, the ability of the human immunodeficiency virus (HIV)-1 Tat and Antennapedia homeodomain proteins to penetrate cells was discovered.[1] Subsequent studies have shown that short, basic peptides corresponding to the RNA-/DNA-binding domains of these proteins were responsible for their translocation into cells, and that the conjugation of various exogenous proteins with these basic peptides allowed their efficient delivery into cells.[2,3] Considerable research has focused on the development of peptides known as cell-penetrating peptides (CPPs) or protein transduction domains (PTDs), which enable the intracellular delivery of bioactive molecules with low membrane permeability.[3–5] In addition to the above-mentioned peptides derived from HIV-1 Tat (TAT peptide)[6] and Antennapedia homeodomain protein (penetratin),[7] oligoarginine,[2,8] transportan,[9] and TP10[10] are the most widely employed CPPs (Figure 1). Using these CPPs, various bioactive and membrane-impermeable molecules possessing different physicochemical properties and molecular weights/sizes have successfully been delivered into cells. One interesting recent application concerns the use of a CPP to enable the introduction of stable isotope-labeled proteins into eukaryotic cells for the investigation of their in vivo conformation and dynamic properties by so-called in-cell NMR.[11]

On the other hand, recent developments in molecular biology and genome science have led to the discovery of a number of disease-related genes. Attempts to apply these findings to the therapy of genetic and acquired diseases, including cancer and viral diseases, are in progress. In addition to gene delivery and antisense therapies, RNA interference (RNAi) is a promising therapeutic methodology. Nucleic acid pharmaceuticals (NAPs) target intracellular molecules; therefore, the development of efficient methods for the intracellular delivery of NAPs, including genes/plasmids, short oligonucleotides (ONs), and small interfering RNAs (siRNAs), and their analogues is necessary.

CPPs have received attention as an attractive means for NAP delivery, not only because of their high internalization ability but also due to their potential for variable structural design. Significant improvements in the design and performance of CPP-based NAP delivery systems have been made in the past few years (see refs 12–15 and those cited therein). In this Account, we summarize current CPP-based NAP delivery approaches, especially self-assembling core–shell NAP nanoparticles comprising stearylated CPPs, and those employing liposome-based multifunctional envelope-type nanodevices (MEND). Their impact on NAP delivery and therapeutic potential is also discussed.

CPPs

HIV-1 TAT:	GRKKRRQRRRPPQ
R8:	RRRRRRRR
penetratin:	RQIKIWFQNRRMKWKK
Transportan:	GWTLNSAGYLLGKINLKALAALAKKIL-amide
TP10:	AGYLLGKINLKALAALAKKIL-amide

STR-CPPs

STR-R8:	stearly-RRRRRRRR-amide
STR-$(RxR)_4$:	stearly-$(RxR)_4$-amide (x=6-aminohexanoic acid)
STR-TP10:	stearyl-AGYLLGKINLKALAALAKKIL-amide
PF6:	stearyl-AGYLLGKINLKALAALAKKIL-amide

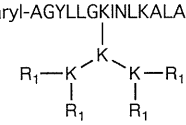

PF14:	stearyl-AGYLLGKLLOOLAAAALOOLL-amide (O=ornithine)
NickFect1:	stearyl-AGY(PO_3)LLGKTNLKALAALAKKIL-amide

stearyl = $CH_3(CH_2)_{16}CO$-

R_1 =

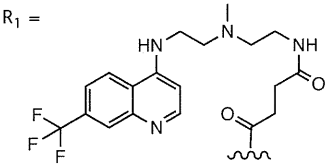

FIGURE 1. Structures of representative CPPs and stearylated CPPs (STR-CCPs).

2. NAP Delivery Using Stearylated CPPs

The original reports on TAT and other CPPs described their potential for the delivery of peptides and proteins into cells.[2–4,6–10,16] The CPPs and their peptide/protein conjugates were internalized into nearly 100% of cells in a few to several tens of minutes and yielded the bioactivity of the intracellularly delivered peptides/proteins; however, covalent protein–CPP conjugation was required for effective delivery. Inspired by these results, attempts have been made to utilize CPPs for the delivery of NAPs (e.g., gene, ON, and siRNA) into cells. These approaches can be divided into two types: the conjugation of NAPs with arginine-rich CPPs and the formation of noncovalent complexes of CPPs and NAPs. However, considering the need for specific conjugation procedures and the easy formation of precipitates of cationic CPPs and negatively charged NAPs, the latter approach is preferred for gene and nucleic acid delivery.

Although reports have described the transfection of plasmid DNAs (pDNAs) into cells in complexes with TAT itself or other unmodified CPPs, delivery was inefficient.[14,17]

Although these approaches yielded somewhat greater gene expression than control (plasmid only) transfection, the improvement in transfection efficiency was not as great as with cationic liposomes (e.g., Lipofectamine) or polymers (e.g., polyethyleneimine).

To improve transfection efficiency, Futaki et al.[18] evaluated the effect of the introduction of a hydrophobic moiety to arginine-rich CPPs. The interaction of these hydrophobic moieties with each other or with nucleobases in the plasmid/CPP complexes may enhance compaction of the pDNA and lead to self-assembling particle formation that will favor NAP delivery in vitro and in vivo. The increased hydrophobicity of the complex may enhance cell surface adsorption and so aid in membrane translocation.

A comparison of the transfection efficiency of N-terminally acylated oligoarginines with variable numbers of arginines and acyl chains, stearyl-octaarginine (STR-R8) was found to have the highest transfection efficiency.[18] Simple mixing of STR-R8 with pDNA yielded a transfection efficacy comparable to that of Lipofectamine with no significant cytotoxicity.[18,19] Atomic force microscopy revealed the effective condensation of pDNA by STR-R8, but not R8, to yield particle-like structures having diameters of ~120 nm and a positive zeta potential (19.3 mV).[19] Therefore, the stearyl moiety in arginine-rich CPPs acts as a hydrophobic core to facilitate the formation of particle structures while maintaining a positive surface charge. This may also lead to enhanced adsorption on cell surfaces and eventual cellular uptake.

STR-R8 was also employed for siRNA delivery. Tönges et al.[20] reported enhanced siRNA transfection into primary hippocampal neurons and the effective induction of siRNA-mediated gene silencing in primary neuron cultures with lower cytotoxicity than a cationic liposome-based transfection agent. A similar approach was reported by Kim et al.,[21] who employed nonaarginine (R9) modified with cholesterol. The siRNA-containing noncovalent cholesteryl-R9 complex targeting vascular endothelial growth factor (VEGF) was not just effective in vitro; local administration in vivo led to tumor regression.

N-Terminal acylation for the compaction of DNA/RNA complexes to stimulate cellular uptake may be applicable to other types of CPPs. TP10 is another representative CPP with a primary amphiphilic, hydrophobic/weakly basic structure developed by Langel and his colleagues.[10] Although the physicochemical properties of this CPP are somewhat different from those of arginine-rich CPPs, the N-terminal stearylation of TP10 (STR-TP10) markedly improved the delivery efficiency of a phosphorothioate 2′-*O*-methyl RNA oligonucleotide (2′-OMe ON) for splice correction into cells.[22] Aberrant pre-mRNA splicing is involved in various diseases, and the blockage of aberrant splice sites by ON derivatives has significant therapeutic potential. However, effective methods for the intracellular delivery of ON derivatives are required to obtain therapeutic effects. The splice correction levels resulting from the use of STR-TP10 were comparable to those obtained with Lipofectamine 2000, and negligible cytotoxicity was observed. Along the same lines, Lehto et al.[23] reported the applicability of an STR-$(RxR)_4$ peptide (x = 6-aminohexanoic acid) for splice correction. The above results suggest that stearylation improved the transfection efficiency of CPPs other than oligoarginines.

Chloroquine is a lysosomotropic agent that induces osmotic swelling and so promotes the disruption of endosomal compartments. Significantly improved splice correction was observed after the treatment of cells with an STR-TP10/2′-OMe ON complex in the presence of chloroquine.[22] However, in terms of future in vivo applications, this strategy is impractical because chloroquine must be taken up with the STR-TP10/NAP complex to obtain improved endosomal escape. PepFect6 (PF6) was thus developed by Langel and his fellow researchers as a novel carrier peptide.[24] PF6 shares the same peptide sequence as STR-TP10 (PepFect 3, PF3); however, four trifluoromethylquinoline moieties are covalently connected to a lysine side chain to improve endosomal escape of the peptide. Even bearing these trifluoromethylquinoline moieties, PF6 formed nanoparticles with siRNA 70−100 nm in diameter in water and 125−200 nm in serum-containing media. As determined by a liposome leakage assay, the PF6/siRNA complex showed an increased membrane destabilization effect at pH 5.5 (endosomal pH) than at pH 7.4, suggesting pH-dependent endosomolytic properties. Effective siRNA delivery was attained into human umbilical vein endothelial cells and Jurkat cells in vitro and in vivo. Intravenous administration of the PF6 complex with siRNA targeting the endogenous hypoxanthine phosphoribosyltransferase 1 (HPRT1) gene resulted in significant reductions in HPRT1 mRNA levels (knockdown efficacy: 50−70%) in the kidneys, lungs, and liver with no significant cytotoxicity.[24] PepFect 14 (PF14) is a novel stearylated peptide that is a modified version of STR-TP10. It was modified with ornithines instead of lysines (in STR-TP10) as a source of positive charge. PepFect 14 can produce solid nanocomplex formulations and yield remarkable splice-correction activity comparable to that from the freshly prepared nanocomplexes in solution.[25] Another

interesting stearylated CPP (NickFect) was reported by Oskolkov et al.,[26] a STR-TP10 analogue having phosphorylated Tyr side chain, yielding an efficient ON delivery vector.

The strategy of attaching a stearyl moiety to form a core–shell structure was also employed by Okada and co-workers.[27,28] A stearylated peptide comprised of cysteine, histidine, and arginine (STR-$CH_2R_4H_2C$) was intended to compact the siRNA with the help of the stearyl moiety and additional disulfide cross-linking between cysteines. Histidine residues may also contribute to endosomal membrane disruption due to a proton sponging effect.[27] STR-$CH_2R_4H_2C$ showed a higher transfection efficacy than Lipofectamine, even in the presence of serum. STR-$CH_2R_4H_2C$ was also employed for in vivo siRNA delivery; the injection of a VEGF-targeting siRNA complexed with this peptide in tumor-bearing mice produced a strong antitumor effect.[28]

Other promising nucleic acid delivery approaches (other than stearylated CPPs) include the 20-residue amphipathic peptide CADY (Ac-GLWRALWRLLRSLWRLLWRA-cysteamide) reported by Divita and co-workers.[29,30] The self-assembly of CADY and siRNA formed a "raspberry"-like particle capable of efficient siRNA delivery in vitro and in vivo. Eguchi et al.[31] reported siRNA delivery using a fusion protein consisting of TAT and a double-stranded RNA-binding domain (Tat-DRBD).

3. NAP Delivery Using CPP-Modified MEND

Stearylated CPPs provide novel methods for the intracellular delivery of NAPs. These approaches have the advantage of easy and simple methods of formulation. On the other hand, various polymer-modified liposomes and macromolecular carriers, including those based on polyethylenimine, chitosan, dendrimers, and nanogels, have been investigated for their potential as nonviral vectors to attain safe and efficient delivery of NAPs into target cells. Of these, polymer-modified liposomes are attractive for NAP delivery and are capable of encapsulating NAPs without the need to alter their chemical structures; moreover, the feasibility of design via surface modification or arrangement of the lipid composition of liposomes gives them another advantage as an NAP delivery vector.[14,15,32] The addition of other targeting moieties (e.g., homing or fusogenic peptides) will enhance the delivery efficiency and biological effects. Biodegradability may reduce the peptides' toxicity and antigenicity. Therefore, ongoing efforts seek to accelerate the cellular uptake of CPP-employing liposomes to obtain greater biological responses.

The first report of CPP-modified liposomes was made by Torchilin and co-workers.[33,34] TAT-modified liposomes using a poly(ethylene glycol) (MW 3000) linker were required to connect the TAT peptide and phosphatidylethanolamine (PE) in order to successfully implant the TAT segment within the liposomal membrane to attain maximum internalization. TAT-liposomes containing a small quantity of a cationic lipid formed noncovalent complexes with DNA and were used for transfection both in vitro and in vivo.

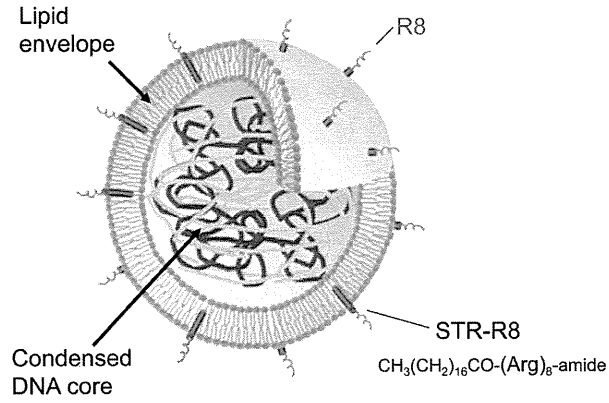

FIGURE 2. Schematic representation of R8-MEND.

Khalil and co-workers[35,36] developed an R8-modified liposome encapsulating pDNA composed of a condensed pDNA core with cationic molecules, including poly-L-lysine, STR-R8, and protamine, coated with a lipid membrane. The modification of liposomes with R8 was easily achieved by the addition of STR-R8 to the liposomal solution, leading to insertion of the stearyl moiety into liposomal membranes.[35] This method of liposome modification (MEND) is compatible with other conventional surface modification methods and thus allows flexible and variable liposome design or "programmed packaging" (Figure 2).[32,35,36] The modification of liposomes with 5 mol % STR-R8 produced the greatest internalization efficacy, attaining a transfection activity as high as that of adenovirus in dividing cells with low cytotoxicity.[36] The in vivo potential of R8-MEND was demonstrated by the topical application of R8-MEND particles containing constitutively active bone morphogenetic protein type IA receptor, which yielded a significant effect on hair growth.[36] R8-MEND is also capable of the efficient delivery of siRNA into cells. Ex vivo siRNA delivery to primary mouse bone marrow-derived dendritic cells, with the eventual aim of developing a cancer vaccine, has been reported.[37,38] The development of ever more sophisticated MEND concepts continues. This includes T-MEND,[39] which has a tetra-lamellar structure (i.e., two nuclear membrane-fusogenic inner envelopes and two endosome-fusogenic outer envelopes) to facilitate stepwise fusion with endosomal and nuclear membranes and efficient DNA delivery

to the nucleus. GALA/PPD-MEND(PPD = poly(ethylene glycol)–peptide–dioleoylphosphatidyl ethanolamine) was developed for cancer targeting, the internalization of which is triggered by matrix metalloproteinase.[40]

4. Internalization Mechanisms of CPPs and Intracellular NAP Delivery

Despite the large number of reports of the successful intracellular delivery of bioactive molecules in vitro and in vivo using CPPs, the precise mechanisms of their internalization remain controversial. One of the reasons for the difficulty in elucidating these mechanisms may be that in many cases CPPs can interact with multiple cell surface molecules, including membrane lipids and membrane-associated proteoglycans. Therefore, it is likely that CPPs can be taken up by cells via multiple pathways, including direct penetration of the plasma membrane and endocytic uptake mediated by clathrin, caveolae, and/or other molecules, depending on the nature of the peptide/cell interaction.[3,13,41,42] Differences in the physicochemical properties of CPPs and cargo molecules also affect their fate after uptake. Elucidation of the cellular uptake mechanisms of CPPs should improve the delivery efficacy of NAPs using CPPs. The most well-studied mechanisms of internalization may be that of arginine-rich CPPs, including TAT and oligoarginine peptides, which share similar methods of internalization.

Whereas both arginine and lysine are representative basic amino acids, oligoarginines generally have a higher internalization efficiency compared with oligolysines possessing the same number of residues. Arginine is a stronger base (pK_a of the guanidino function: ~12.5) than lysine (pK_a of the ε-amino function: ~10.5), while many other cationic nucleic acid carriers are even weaker bases that utilize the proton sponge effect to promote endosomal escape.[43] In addition, the guanidino function may form two hydrogen bonds with phosphate, sulfate, and carboxylate in cell-membrane-associated molecules (e.g., lipids and glycosaminoglycans) (Figure 3), whereas lysine can form only one hydrogen bond with these groups. Whether the difference in basicity or the ability to form hydrogen bonds is a stronger determinant of cellular uptake efficacy is debatable. Rothbard et al.[44] showed the importance of hydrogen bond formation in the superiority of arginine over lysine in an elegant study using N^G-methyl arginine; methylation of the guanidine function should increase the basicity and diminish the hydrogen bond formation capacity. The cellular uptake of octamethylarginine was only ~20% that of nonmethylated R8, indicating the importance of hydrogen bond formation in the cellular uptake of arginine-rich CPPs. Sakai et al.[45] and Rothbard et al.[44] also suggested the possibility of hydrogen bond formation by

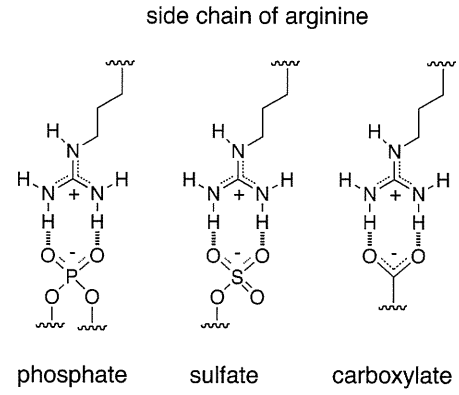

FIGURE 3. Possible mode of hydrogen bond formation between arginine and membrane-associated functional groups.

oligoarginine peptides containing hydrophobic counteranions such as phosphatidylglycerol and lauric acid; these may also assist in the translocation of oligoarginines through membranes. Similarly, enhanced internalization of arginine-rich CPPs and complex formation with splice-switching ONs in the presence of a hydrophobic counteranion, pyrenebutyrate, has been reported.[46–48] These results suggest that arginine promotes cellular uptake more efficiently than lysine due to its hydrogen bond formation capacity.

While the feasibility of direct membrane penetration by oligoarginine CPPs and conjugates has been suggested, especially when attached to relatively small cargo molecules (MW $<\sim$2000),[4,42,49] endocytosis is considered to be the dominant cellular uptake pathway for intracellular NAP delivery using CPPs. For the cellular uptake of arginine-rich CPPs and their NAP conjugates, membrane-associated proteoglycans, including heparan or chondroitin sulfate proteoglycans, play a role in the accumulation of these molecules on cell surfaces via an interaction between the guanidino function of arginine and sulfates in the proteoglycans.[50,51] Nakase et al.[52] and others[53] have proposed that macropinocytosis, accompanied by actin reorganization, plasma membrane ruffling, and the stimulated engulfment of large volumes of extracellular fluid, serves as a major pathway of endocytosis for arginine-rich CPPs (Figure 4). Macropinocytosis does not usually operate in cells; it is activated only when specific stimuli (e.g., growth factors or viruses) are applied.[54] Nakase and co-workers[51,55] suggested that membrane-associated proteoglycans serve as the primary receptor to induce macropinocytosis. Therefore, the interaction of arginine-rich CPPs and their cargos with membrane-associated proteoglycans leads not only to their accumulation on the cell surface but also to the induction of macropinocytosis to accelerate their uptake. The diameters of these macropinosomes are much greater ($>\sim 1\ \mu$m) than those for clathrin- or

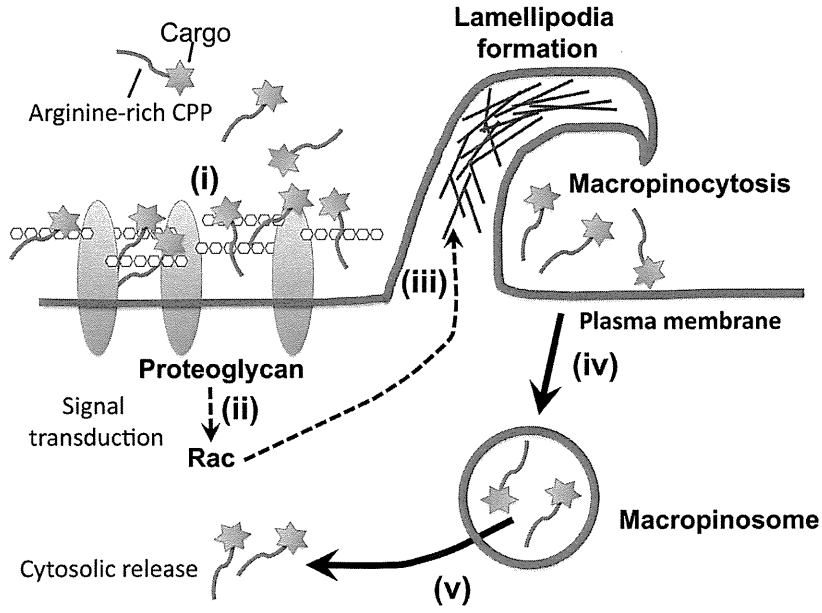

FIGURE 4. Proposed methods for the intracellular delivery of bioactive cargos using arginine-rich CPPs. (i) The interaction of arginine-rich CPPs with membrane-associated proteoglycans leads to (ii) Rac activation, and (iii) actin reorganization, lamellipodia formation, and the induction of macropinocytosis. (iv) Cellular uptake and (v) cytosolic release of the cargos from macropinosomes lead to exertion of their bioactivity.

caveolae-mediated endocytosis (~120 and 80 nm, respectively),[56] which may allow easier cellular uptake of nanoparticles, including R8-MEND. This may be another advantage of arginine-rich CPPs for intracellular NAP delivery.

Studies of the internalization mechanism of arginine-rich peptides have implications for the method of uptake of R8-modified MEND. R8-MEND also binds electrostatically to negatively charged proteoglycans on the cell surface. The methods of cellular uptake of R8-MEND vary depending on the density of arginine. R8-MEND containing 5 mol % STR-R8 liposomal lipids implanted on the surface was taken up by cells via macropinocytosis, whereas that bearing 0.5 mol % STR-R8 was taken up predominantly through clathrin-mediated endocytosis.[35] This result is in agreement with the previous finding that increased clustering of arginine on the cell surface facilitated macropinocytosis and stimulated the uptake of arginine-rich peptides.[52,55] It was also found that the macropinocytic uptake of R8-MEND modified with 5 mol % STR-R8 suffered from less lysosomal degradation than uptake modified with 0.5 mol % STR-R8 via clathrin-mediated endocytosis.[35,57] Thus, optimization of the conditions for macropinocytosis should lead to the mechanism-based design of NAP delivery, resulting in enhanced cellular uptake and bioactivity.

5. Conclusions

The use of arginine-rich CPPs has various implications for NAP delivery into cells. Stearylation of these peptides may lead to the formation of self-assembling nanoparticles with NAP-containing core–shell structures and facilitate cellular uptake. As in the case of PF6, modification with accelerating agents for endosomal escape may further improve the transfection efficiency. Stearylated arginine-rich CPPs are not only useful for the compaction of NAPs, they can be easily applied to the surface modification of liposomes with CPPs, as was shown for R8-MEND. Modification of the liposomal surface charge density may alter the method of cellular uptake, again as found for R8-MEND. Since the activation of macropinocytosis stimulates cellular uptake of extracellular fluid, leading to engulfment into a large endosome (macropinosomes), strategies aimed at stimulating macropinocytosis may stimulate cellular uptake of liposomes and other nanoparticles. Therefore, CPPs provide a platform for the design of efficient intracellular NAP delivery systems. A greater understanding of cellular uptake mechanisms should also contribute to further improvements in delivery systems, and the concepts of core–shell particle formation and MEND may assist in their rational design.

This work was supported in part by Grants-in-Aid for Scientific Research from the Ministry of Education, Culture, Sports, Science and Technology of Japan (to I.N., H.A., K.K., H.H., and S.F.). This study was also supported by the Swedish Research Council, the Swedish Foundation for Strategic Research and VINNOVA (Project No. MDB09-0015) (to Ü.L. and A.G.), and Strategic

Japanese-Swedish Cooperative Programme on "Multidisciplinary BIO" from Japan Science, Technology Agency (JST) and VINNOVA (to S.F.).

BIOGRAPHICAL INFORMATION

Ikuhiko Nakase obtained his Ph.D. in 2005 from Kyoto University. He completed his postdoctoral training at the Department of Chemistry, University of Washington (Seattle, WA). He has been an Assistant Professor of Biochemistry at the Institute for Chemical Research, Kyoto University, since 2006. His research interests include peptide–membrane interactions in cells.

Hidetaka Akita is an Associate Professor of Pharmaceutics in the Laboratory of Molecular Design of Pharmaceutics, Faculty of Pharmaceutical Sciences, Hokkaido University. His main research interest is development of gene delivery system for functional nucleic acids by controlling a intracellular trafficking.

Kentaro Kogure obtained his Ph.D. in 1994 from the University of Tokushima. Following his appointment as a Research Associate at Toyama Medical and Pharmaceutical University, he developed his academic career at the University of Tokushima and Hokkaido University. He has been a full Professor of Biophysical Chemistry at Kyoto Pharmaceutical University since 2007.

Astrid Gräslund received her Ph.D. in biophysics in 1974 from Stockholm University. After serving as a Research Associate and Associate Professor in Biophysics at Stockholm University, she moved to Umea University as Professor of Medical Biophysics in 1988. Since 1993 she has been a Professor of Biophysics at Stockholm University.

Ülo Langel is a Professor and Chairman of the Department of Neurochemistry, Stockholm University. His professional experience includes positions at Tartu University (now Adjunct Professor); the Scripps Research Institute (now Adjunct Professor); and Ljubljana University (now Honorary Professor).

Hideyoshi Harashima is a Professor of Pharmaceutics and chair of the Laboratory of Molecular Design of Pharmaceutics, Faculty of Pharmaceutical Sciences, Hokkaido University. He served as vice president of the Association of Pharmaceutical Science and Technology of Japan (2008–2010). He also serves as a Co-Chair of SIG (Pharmaceutical Biotechnology) of FIP.

Shiroh Futaki obtained his Ph.D. in 1989 from Kyoto University. Following his appointment as a Research Associate and Associate Professor at the University of Tokushima, he moved to Kyoto University in 1997. Meanwhile, he spent 16 months (1989–1991) in the United States as a Postdoctoral Associate in the Department of Biochemistry, Rockefeller University (New York City, NY). He has been a full Professor of Biochemistry at the Institute for Chemical Research, Kyoto University, since 2005.

FOOTNOTES

*To whom correspondence should be addressed.

REFERENCES

1 Dupont, E.; Prochiantz, A.; Joliot, A. Penetratin Story: an Overview. *Methods Mol. Biol.* **2011**, *683*, 21–29.

2 Futaki, S.; Suzuki, T.; Ohashi, W.; Yagami, T.; Tanaka, S.; Ueda, K.; Sugiura, Y. Arginine-Rich Peptides. An Abundant Source of Membrane-Permeable Peptides Having Potential as Carriers for Intracellular Protein Delivery. *J. Biol. Chem.* **2001**, *276*, 5836–5840.

3 Nakase, I.; Takeuchi, T.; Tanaka, G.; Futaki, S. Methodological and Cellular Aspects That Govern the Internalization Mechanisms of Arginine-Rich Cell-Penetrating Peptides. *Adv. Drug Delivery Rev.* **2008**, *60*, 598–607.

4 Wender, P. A.; Galliher, W. C.; Goun, E. A.; Jones, L. R.; Pillow, T. H. The Design of Guanidinium-Rich Transporters and Their Internalization Mechanisms. *Adv. Drug Delivery Rev.* **2008**, *60*, 452–472.

5 *Cell-Penetrating Peptides. Methods and Protocols*; Langel, Ü., Ed.; Humana Press: New York, 2011.

6 Vivès, E.; Brodin, P.; Lebleu, B. A Truncated HIV-1 Tat Protein Basic Domain Rapidly Translocates Through the Plasma Membrane and Accumulates in the Cell Nucleus. *J. Biol. Chem.* **1997**, *272*, 16010–16017.

7 Derossi, D.; Joliot, A. H.; Chassaing, G.; Prochiantz, A. The Third Helix of the Antennapedia Homeodomain Translocates through Biological Membranes. *J. Biol. Chem.* **1994**, *269*, 10444–10450.

8 Rothbard, J. B.; Garlington, S.; Lin, Q.; Kirschberg, T.; Kreider, E.; McGrane, P. L.; Wender, P. A.; Khavari, P. A. Conjugation of Arginine Oligomers to Cyclosporin A Facilitates Topical Delivery and Inhibition of Inflammation. *Nat. Med.* **2000**, *6*, 1253–1257.

9 Pooga, M.; Hällbrink, M.; Zorko, M.; Langel, Ü. Cell Penetration by Transportan. *FASEB J.* **1998**, *12*, 67–77.

10 Soomets, U.; Lindgren, M.; Gallet, X.; Hällbrink, M.; Elmquist, A.; Balaspiri, L.; Zorko, M.; Pooga, M.; Brasseur, R.; Langel, U. Deletion Analogues of Transportan. *Biochem. Biophys. Acta* **2000**, *1467*, 165–176.

11 Inomata, K.; Ohno, A.; Tochio, H.; Isogai, S.; Tenno, T.; Nakase, I.; Takeuchi, T.; Futaki, S.; Ito, Y.; Hiroaki, H.; Shirakawa, M. High-Resolution Multi-Dimensional NMR Spectroscopy of Proteins in Human Cells. *Nature* **2009**, *458*, 106–109.

12 Deshayes, S.; Konate, K.; Aldrian, G.; Crombez, L.; Heitz, F.; Divita, G. Structural Polymorphism of Non-Covalent Peptide-Based Delivery Systems: Highway to Cellular Uptake. *Biochim. Biophys. Acta* **2010**, *1798*, 2304–2314.

13 Said Hassane, F.; Saleh, A. F.; Abes, R.; Gait, M. J.; Lebleu, B. Cell Penetrating Peptides: Overview and Applications to the Delivery of Oligonucleotides. *Cell. Mol. Life Sci.* **2010**, *67*, 715–726.

14 Khalil, I. A.; Kogure, K.; Futaki, S.; Harashima, H. Octaarginine-Modified Liposomes: Enhanced Cellular Uptake and Controlled Intracellular Trafficking. *Int. J. Pharm.* **2008**, *354*, 39–48.

15 Hatakeyama, H.; Akita, H.; Harashima, H. A Multifunctional Envelope Type Nano Device (MEND) for Gene Delivery to Tumors Based on the EPR Effect: a Strategy for Overcoming the PEG Dilemma. *Adv. Drug Delivery Rev.* **2011**, *63*, 152–160.

16 Fawell, S.; Seery, J.; Daikh, Y.; Moore, C.; Chen, L. L.; Pepinsky, B.; Barsoum, J. Tat-Mediated Delivery of Heterologous Proteins into Cells. *Proc. Natl. Acad. Sci. U.S.A.* **1994**, *91*, 664–668.

17 Mann, A.; Thakur, G.; Shukla, V.; Singh, A. K.; Khanduri, R.; Naik, R.; Jiang, Y.; Kalra, N.; Dwarakanath, B. S.; Langel, U.; Ganguli, M. Differences in DNA Condensation and Release by Lysine and Arginine Homopeptides Govern Their DNA Delivery Efficiencies. *Mol. Pharmaceutics* **2011**, *8*, 1729–1741.

18 Futaki, S.; Ohashi, W.; Suzuki, T.; Niwa, M.; Tanaka, S.; Ueda, K.; Harashima, H.; Sugiura, Y. Stearylated Arginine-Rich Peptides: a New Class of Transfection Systems. *Bioconjugate Chem.* **2001**, *12*, 1005–1011.

19 Khalil, I. A.; Futaki, S.; Niwa, M.; Baba, Y.; Kaji, N.; Kamiya, H.; Harashima, H. Mechanism of Improved Gene Transfer by the N-Terminal Stearylation of Octaarginine: Enhanced Cellular Association by Hydrophobic Core Formation. *Gene Ther.* **2004**, *11*, 636–644.

20 Tönges, L.; Lingor, P.; Egle, R.; Dietz, G. P. H; Fahr, A.; Bähr, M. Stearylated Octaarginine and Artificial Virus-Like Particles for Transfection of siRNA into Primary Rat Neurons. *RNA* **2006**, *12*, 1431–1438.

21 Kim, W. J.; Christensen, L. V.; Jo, S.; Yockman, J. W.; Jeong, J. H.; Kim, Y. H.; Kim, S. W. Cholesteryl Oligoarginine Delivering Vascular Endothelial Growth Factor siRNA Effectively Inhibits Tumor Growth in Colon Adenocarcinoma. *Mol. Ther.* **2006**, *14*, 343–350.

22 Mäe, M.; El Andaloussi, S.; Lundin, P.; Oskolkov, N.; Johansson, H. J.; Guterstam, P.; Langel, U. A Stearylated CPP for Delivery of Splice Correcting Oligonucleotides Using a Non-Covalent Co-Incubation Strategy. *J. Controlled Release* **2009**, *134*, 221–227.

23 Lehto, T.; Abes, R.; Oskolkov, N.; Suhorutsenko, J.; Copolovici, D. M.; Mäger, I.; Viola, J. R.; Simonson, O. E.; Ezzat, K.; Guterstam, P.; Eriste, E.; Smith, C. I.; Lebleu, B.; El Andaloussi, S.; Langel, U. Delivery of Nucleic Acids with a Stearylated $(RxR)_4$ Peptide Using a Non-Covalent Co-Incubation Strategy. *J. Controlled Release* **2010**, *141*, 42–51.

24 El Andaloussi, S.; Lehto, T.; Mäger, I.; Rosenthal-Aizman, K.; Oprea, I. I.; Simonson, O. E.; Sork, H.; Ezzat, K.; Copolovici, D. M.; Kurrikoff, K.; Viola, J. R.; Zaghloul, E. M.; Sillard, R.; Johansson, H. J.; Said Hassane, F.; Guterstam, P.; Suhorutšenko, J.; Moreno, P. M.; Oskolkov, N.; Hälldin, J.; Tedebark, U.; Metspalu, A.; Lebleu, B.; Lehtiö, J.; Smith, C. I.; Langel, U. Design of a Peptide-Based Vector, PepFect6, for Efficient Delivery of siRNA in Cell Culture and Systemically in Vivo. *Nucleic Acids Res.* **2011**, *39*, 3972–3987.

25 REzzat, K.; EL Andaloussi, S.; Zaghloul, E. M.; Lehto, T.; Lindberg, S.; Moreno, P. M.; Viola, J. R.; Magdy, T.; Abdo, R.; Guterstam, P.; Sillard, R.; Hammond, S. M.; Wood, M. J.; Arzumanov, A. A.; Gait, M. J.; Smith, C. I.; Hällbrink, M.; Langel, Ü. PepFect 14, a Novel Cell-Penetrating Peptide for Oligonucleotide Delivery in Solution and as Solid Formulation. *Nucleic Acids Res.* **2011**, *39*, 5284–5298.

26 Oskolkov, N.; Arukuusk, P.; Copolovici, D. M.; Lindberg, S.; Margus, H.; Padari, K.; Pooga, M.; Langel, Ü. NickFects, Phosphorylated Derivatives of Transportan 10 for Cellular Delivery of Oligonucleotides. *Int. J. Pept. Res. Ther.* **2011**, *17*, 147–157.

27 Tanaka, K.; Kanazawa, T.; Ogawa, T.; Takashima, Y.; Fukuda, T.; Okada, H. Disulfide Crosslinked Stearoyl Carrier Peptides Containing Arginine and Histidine Enhance siRNA Uptake and Gene Silencing. *Int. J. Pharm.* **2010**, *398*, 219–224.

28 Tanaka, K.; Kanazawa, T.; Ogawa, T.; Suda, Y.; Takashima, Y.; Fukuda, T.; Okada, H. A Novel, Bio-Reducible Gene Vector Containing Arginine and Histidine Enhances Gene Transfection and Expression of Plasmid DNA. *Chem. Pharm. Bull.* **2011**, *59*, 202–207.

29 Crombez, L.; Divita, G. A Non-Covalent Peptide-Based Strategy for siRNA Delivery. *Methods Mol. Biol.* **2011**, *683*, 349–360.

30 Crombez, L.; Morris, M. C.; Heitz, F.; Divita, G. A Non-Covalent Peptide-Based Strategy for ex Vivo and in Vivo Oligonucleotide Delivery. *Methods Mol. Biol.* **2011**, *764*, 59–73.

31 Eguchi, A.; Meade, B. R.; Chang, Y. C.; Fredrickson, C. T.; Willert, K.; Puri, N.; Dowdy, S. F. Efficient siRNA Delivery into Primary Cells by a Peptide Transduction Domain-dsRNA Binding Domain Fusion Protein. *Nat. Biotechnol.* **2009**, *27*, 567–571.

32 Kogure, K.; Akita, H.; Yamada, Y.; Harashima, H. Multifunctional Envelope-Type Nano Device (MEND) as a Non-Viral Gene Delivery System. *Adv. Drug Delivery Rev.* **2008**, *60*, 559–571.

33 Torchilin, V. P.; Rammohan, R.; Weissig, V.; Levchenko, T. S. TAT Peptide on the Surface of Liposomes Affords Their Efficient Intracellular Delivery Even at Low Temperature and in the Presence of Metabolic Inhibitors. *Proc. Natl. Acad. Sci. U.S.A.* **2001**, *98*, 8786–8791.

34 Torchilin, V. P.; Levchenko, T. S.; Rammohan, R.; Volodina, N.; Papahadjopoulos-Sternberg, B.; D'Souza, G. G. Cell Transfection in Vitro and in Vivo with Nontoxic TAT Peptide-Liposome-DNA Complexes. *Proc. Natl. Acad. Sci. U.S.A.* **2003**, *100*, 1972–1977.

35 Khalil, I. A.; Kogure, K.; Futaki, S.; Harashima, H. High Density of Octaarginine Stimulates Macropinocytosis Leading to Efficient Intracellular Trafficking for Gene Expression. *J. Biol. Chem.* **2006**, *281*, 3544–3551.

36 Khalil, I. A.; Kogure, K.; Futaki, S.; Hama, S.; Akita, H.; Ueno, M.; Kishida, H.; Kudoh, M.; Mishina, Y.; Kataoka, K.; Yamada, M.; Harashima, H. Octaarginine-Modified Multifunctional Envelope-Type Nanoparticles for Gene Delivery. *Gene Ther.* **2007**, *14*, 682–689.

37 Nakamura, Y.; Kogure, K.; Futaki, S.; Harashima, H. Octaarginine-Modified Multifunctional Envelope-Type Nano Device for siRNA. *J. Controlled Release* **2007**, *119*, 360–367.

38 Akita, H.; Kogure, K.; Moriguchi, R.; Nakamura, Y.; Higashi, T.; Nakamura, T.; Serada, S.; Fujimoto, M.; Naka, T.; Futaki, S.; Harashima, H. Nanoparticles for ex Vivo siRNA Delivery to Dendritic Cells for Cancer Vaccines: Programmed Endosomal Escape and Dissociation. *J. Controlled Release* **2010**, *143*, 311–317.

39 Akita, H.; Kudo, A.; Minoura, A.; Yamaguti, M.; Khalil, I. A.; Moriguchi, R.; Masuda, T.; Danev, R.; Nagayama, K.; Kogure, K.; Harashima, H. Multi-Layered Nanoparticles for Penetrating the Endosome and Nuclear Membrane via a Step-Wise Membrane Fusion Process. *Biomaterials* **2009**, *30*, 2940–2949.

40 Hatakeyama, H.; Akita, H.; Ito, E.; Hayashi, Y.; Oishi, M.; Nagasaki, Y.; Danev, R.; Nagayama, K.; Kaji, N.; Kikuchi, H.; Baba, Y.; Harashima, H. Systemic Delivery of siRNA to Tumors Using a Lipid Nanoparticle Containing a Tumor-Specific Cleavable PEG-Lipid. *Biomaterials* **2011**, *32*, 4306–4316.

41 Duchardt, F.; Fotin-Mleczek, M.; Schwarz, H.; Fischer, R.; Brock, R. A Comprehensive Model for the Cellular Uptake of Cationic Cell-Penetrating Peptides. *Traffic* **2007**, *8*, 848–866.

42 Jones, A. T. Gateways and Tools for Drug Delivery: Endocytic Pathways and the Cellular Dynamics of Cell Penetrating Peptides. *Int. J. Pharm.* **2008**, *354*, 34–38.

43 Zuber, G.; Dauty, E.; Nothisen, M.; Belguise, P.; Behr, J. P. Towards Synthetic Viruses. *Adv. Drug. Delivery Rev.* **2001**, *52*, 245–253.

44 Rothbard, J. B.; Jessop, T. C.; Lewis, R. S.; Murray, B. A.; Wender, P. A. Role of Membrane Potential and Hydrogen Bonding in the Mechanism of Translocation of Guanidinium-Rich Peptides into Cells. *J. Am. Chem. Soc.* **2004**, *126*, 9506–9507.

45 Sakai, N.; Takeuchi, T.; Futaki, S.; Matile, S. Direct Observation of Anion-Mediated Translocation of Fluorescent Oligoarginine Carriers into and Across Bulk Liquid and Anionic Bilayer Membranes. *ChemBioChem* **2005**, *6*, 114–122.

46 Perret, F.; Nishihara, M.; Takeuchi, T.; Futaki, S.; Lazar, A. N.; Coleman, A. W.; Sakai, N.; Matile, S. Anionic Fullerenes, Calixarenes, Coronenes, and Pyrenes as Activators of Oligo/Polyarginines in Model Membranes and Live Cells. *J. Am. Chem. Soc.* **2005**, *127*, 1114–1115.

47 Takeuchi, T.; Kosuge, M.; Tadokoro, A.; Sugiura, Y.; Nishi, M.; Kawata, M.; Sakai, N.; Matile, S.; Futaki, S. Direct and Rapid Cytosolic Delivery Using Cell-Penetrating Peptides Mediated by Pyrenebutyrate. *ACS Chem. Biol.* **2006**, *1*, 299–303.

48 Guterstam, P.; Madani, F.; Hirose, H.; Takeuchi, T.; Futaki, S.; El Andaloussi, S.; Gräslund, A.; Langel, Ü. Elucidating Cell-Penetrating Peptide Mechanisms of Action for Membrane Interaction, Cellular Uptake, and Translocation Utilizing the Hydrophobic Counter-Anion Pyrenebutyrate. *Biochim. Biophys. Acta* **2009**, *1788*, 2509–2517.

49 Kosuge, M.; Takeuchi, T.; Nakase, I.; Jones, A. T.; Futaki, S. Cellular Internalization and Distribution of Arginine-Rich Peptides as a Function of Extracellular Peptide Concentration, Serum, and Plasma Membrane Associated Proteoglycans. *Bioconjugate Chem.* **2008**, *19*, 656–664.

50 Suzuki, T.; Futaki, S.; Niwa, M.; Tanaka, S.; Ueda, K.; Sugiura, Y. Possible Existence of Common Internalization Mechanisms Among Arginine-Rich Peptides. *J. Biol. Chem.* **2002**, *277*, 2437–2443.

51 Nakase, I.; Tadokoro, A.; Kawabata, N.; Takeuchi, T.; Katoh, H.; Hiramoto, K.; Negishi, M.; Nomizu, M.; Sugiura, Y.; Futaki, S. Interaction of Arginine-Rich Peptides with Membrane-Associated Proteoglycans Is Crucial for Induction of Actin Organization and Macropinocytosis. *Biochemistry* **2007**, *46*, 492–501.

52 Nakase, I.; Niwa, M.; Takeuchi, T.; Sonomura, K.; Kawabata, N.; Koike, Y.; Takehashi, M.; Tanaka, S.; Ueda, K.; Simpson, J. C.; Jones, A. T.; Sugiura, Y.; Futaki, S. Cellular Uptake of Arginine-Rich Peptides: Roles for Macropinocytosis and Actin Rearrangement. *Mol. Ther.* **2004**, *10*, 1011–1022.

53 Wadia, J. S.; Stan, R. V.; Dowdy, S. F. Transducible TAT-HA Fusogenic Peptide Enhances Escape of TAT-Fusion Proteins after Lipid Raft Macropinocytosis. *Nat. Med.* **2004**, *10*, 310–315.

54 Mercer, J.; Helenius, A. Virus Entry by Macropinocytosis. *Nat. Cell Biol.* **2009**, *11*, 510–520.

55 Nakase, I.; Hirose, H.; Tanaka, G.; Tadokoro, A.; Kobayashi, S.; Takeuchi, T.; Futaki, S. Cell-Surface Accumulation of Flock House Virus-Derived Peptide Leads to Efficient Internalization via Macropinocytosis. *Mol. Ther.* **2009**, *17*, 1868–1876.

56 Swanson, J. A. Shaping Cups into Phagosomes and Macropinosomes. *Nat. Rev. Mol. Cell Biol.* **2008**, *9*, 639–649.

57 El-Sayed, A.; Khalil, I. A.; Kogure, K.; Futaki, S.; Harashima, H. Octaarginine- and Octalysine-Modified Nanoparticles Have Different Modes of Endosomal Escape. *J. Biol. Chem.* **2008**, *283*, 23450–23461.

Transient Focal Membrane Deformation Induced by Arginine-rich Peptides Leads to Their Direct Penetration into Cells

Hisaaki Hirose[1], Toshihide Takeuchi[1,5], Hiroko Osakada[2], Sílvia Pujals[1], Sayaka Katayama[1], Ikuhiko Nakase[1], Shouhei Kobayashi[2], Tokuko Haraguchi[2–4] and Shiroh Futaki[1]

[1]Institute for Chemical Research, Kyoto University, Kyoto, Japan; [2]Advanced ICT Research Institute Kobe, National Institute of Information and Communications Technology, Hyogo, Japan; [3]Graduate School of Frontier Biosciences, Osaka University, Osaka, Japan; [4]Graduate School of Science, Osaka University, Osaka, Japan; [5]Present address: National Institute of Neuroscience, National Center of Neurology and Psychiatry, Tokyo, Japan

Endocytosis has been implicated in the cellular uptake of arginine-rich, cell-penetrating peptides (CPPs). However, accumulating evidence suggests that certain conditions allow the direct, non-endocytic penetration of arginine-rich peptides through the plasma membrane. We previously showed that Alexa Fluor 488-labeled dodeca-arginine (R12-Alexa488) directly enters cells at specific sites on the plasma membrane and subsequently diffuses throughout cells. In this study, we found that the peptide influx was accompanied by the formation of unique, "particle-like" multivesicular structures on the plasma membrane, together with topical inversion of the plasma membrane. Importantly, the conjugation of dodeca-arginine (R12) to Alexa Fluor 488 or a peptide tag derived from hemagglutinin (HAtag) significantly accelerated particle formation, suggesting that the chemical properties of the attached molecules (cargo molecules) may contribute to translocation of the R12 peptide. Coincubation with R12-HAtag allowed the membrane-impermeable R4-Alexa488 to permeate cells. These results suggest that R12 peptides attached to hydrophobic cargo molecules stimulate dynamic morphological alterations in the plasma membrane, and that these structural changes allow the peptides to permeate the plasma membrane. These findings may provide a novel mode of cell permeabilization by arginine-rich peptides as a means of drug delivery.

Received 7 September 2011; accepted 26 December 2011; advance online publication 14 February 2012. doi:10.1038/mt.2011.313

INTRODUCTION

Intracellular delivery using cell-penetrating peptides (CPPs; also known as protein transduction domains) has received major attention as a novel method of efficiently introducing exogenous molecules into cells.[1,2] Among them, arginine-rich peptides including oligoarginine and HIV-1 Tat (48–60) are regarded as one of the representative classes of CPPs that facilitates efficient translocation through biological membranes.[3–8] However, the detailed membrane translocation mechanisms of these peptides are still being debated. Recent studies using intact living cells showed endocytic pathways including macropinocytosis to be major routes for internalization of these peptides.[9–14] However, accumulating evidence indicates that the internalization mechanisms of arginine-rich peptides differ according to the administration conditions (e.g., peptide sequence, peptide concentration, cell type, and culture medium) and that endocytosis may not be the sole mechanism of internalization of arginine-rich peptides.[14–16] Studies by us and others on cellular localization using fluorescently labeled arginine-rich peptides have shown that octa-arginine (R8) and Tat peptides yield diffuse signals when applied to cells at a temperature of 4 °C in the presence of endocytosis inhibitors including 5-(*N*-ethyl-*N*-isopropyl)amiloride (EIPA) and methyl-β-cyclodextrin, while maintaining membrane integrity.[15,16] The endocytic uptake of these peptides would yield endosome-like punctate signals in the cytoplasm. The diffuse signals from the internalized peptides under endocytosis-suppressing conditions are instead highly suggestive of the presence of direct translocation pathways.

More recently, we conducted a detailed study on the relationship between administered concentration and eventual cellular localization of dodeca-arginine (R12), a peptide that should interact more strongly with cell surface molecules than R8 or Tat.[16] At relatively low concentrations, R12 labels endosome-like structures, yielding punctate signals similar to those for R8 and Tat peptides. When the peptide concentration exceeds a certain threshold, however, diffuse cytosolic labeling for R12 was predominantly observed, which was accompanied by a dramatic increase in overall cellular fluorescence. The mechanism involved cannot be simple passive diffusion through the lipid bilayer because the diffusion is only initiated at specific sites on the plasma membranes.[16]

In the present study, using an Alexa Fluor 488-labeled R12 peptide (R12-Alexa488), whose Alexa Fluor 488 moiety (molecular weight ~700) can be regarded as a model of low-molecular-weight cargo molecules, we showed that interaction with the peptide caused dynamic structural alterations in the plasma membrane and induced the formation of unique "particle-like" structures composed of multiple vesicles on the plasma membrane, together

The first two authors equally contributed to this work.

Correspondence: *Shiroh Futaki, Institute for Chemical Research, Kyoto University, Uji, Kyoto 611-0011, Japan. E-mail: futaki@scl.kyoto-u.ac.jp*